PHILOSOPHICAL TRANSACTIONS OF THE ROYAL SOCIETY A MATHEMATICAL, PHYSICAL & ENGINEERING SCIENCES

Continuous Elastic Phase Transitions in Pure and Disordered Crystals

Franz Schwabl and Uwe Claus Tauber

Phil. Trans. R. Soc. Lond. A 1996 **354**, 2847-2873
doi: 10.1098/rsta.1996.0132

Continuous elastic phase transitions in pure and disordered crystals

By Franz Schwabl[1] and Uwe Claus Täuber[1,2]†

[1]*Institut für Theoretische Physik, Physik–Department der TU München, James–Franck–Straße, D–85747 Garching, Germany*

[2]*Lyman Laboratory of Physics, Harvard University, Cambridge, MA 02138, USA*

We review the theory of second-order (ferro-)elastic phase transitions, where the order parameter consists of a certain linear combination of strain tensor components, and the accompanying soft mode is an acoustic phonon. In three-dimensional crystals, the softening can occur in one- or two-dimensional soft sectors. The ensuing anisotropy reduces the effect of fluctuations, rendering the critical behaviour of these systems classical for a one-dimensional soft sector, and classical with logarithmic corrections in the case of a two-dimensional soft sector. The dynamical critical exponent is $z = 2$, and as a consequence the sound velocity vanishes as $c_s \propto |T - T_c|^{1/2}$, while the phonon damping coefficient is essentially temperature-independent. Even if the elastic phase transition is driven by the softening of an optical mode linearly coupled to a transverse acoustic phonon, the critical exponents retain their mean-field values. Disorder may lead to a variety of precursor effects and modified critical behaviour. Defects that locally soften the crystal may induce the phenomenon of local order parameter condensation. When the correlation length of the pure system exceeds the average defect separation $n_D^{-1/3}$, a disorder-induced phase transition to a state with non-zero average order parameter can occur at a temperature $T_c(n_D)$ well above the transition temperature T_c^0 of the pure crystal. Near T_c^0, the order-parameter curve, susceptibility, and specific heat appear rounded. For $T < T_c(n_D)$ the spatial inhomogeneity induces a static central peak with finite q width in the scattering cross section, accompanied by a dynamical component that is confined to the very vicinity of the disorder-induced phase transition.

1. Introduction

Generally, displacive structural phase transformations (for reviews, see Bruce & Cowley (1981) and Rao & Rao (1987)) can be divided into two different groups, namely distortive and elastic phase transitions. At distortive phase transitions some of the ions or molecular groups in the crystal's elementary cell are displaced with respect to each other. The corresponding displacement field serves as an appropriate order parameter for the transition, which in the case of a second-order transition is thus characterized by the softening of an optical phonon mode that becomes overdamped

† Present address: Department of Physics and Theoretical Physics, University of Oxford, 1 Keble Road, Oxford OX1 3NP, UK.

Phil. Trans. R. Soc. Lond. A (1996) **354**, 2847–2873
Printed in Great Britain

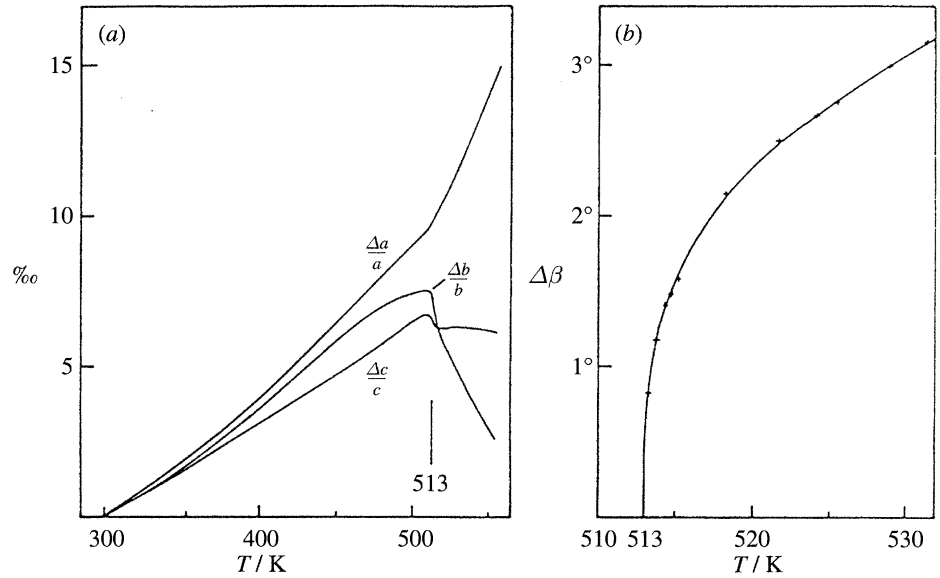

Figure 1. Temperature dependence of the lattice parameters (a) and the monoclinic angle β (b) in NaOH (from Bleif *et al.* 1971).

in the vicinity of the transition. Ionic displacements may lead to the appearance of a macroscopic polarization, i.e. to ferro- or antiferroelectric behaviour. Famous examples of this group of structural phase transitions are the perovskites with the high-temperature simple-cubic ABO_3 crystal structure; e.g. the ferroelectric $BaTiO_3$, the antiferroelectric $NaNbO_3$, and $SrTiO_3$, which displays an antiferrodistortive transition accompanied by the softening of a zone-boundary phonon (see Lüthi & Rehwald 1981). At these distortive transformations the elastic degrees of freedom constitute merely secondary variables, their interaction with the critical order parameter fluctuations being quadratic in the order parameter and linear in the strains.

At an elastic phase transition (also called ferroelastic), on the other hand, the crystallographic unit cell undergoes an elastic deformation, as is depicted in figure 1 for NaOH (for a review, see Wadhawan 1982). Thus the order parameter in this case is a certain linear combination of appropriate components of the strain tensor. In the majority of cases the crystal undergoes a shear deformation, and the accompanying soft mode is the corresponding transverse acoustic phonon. KH_2PO_4 (KDP), KCN, and Fe_3O_4, for example, display a first-order elastic phase transformation, while in K-Na-tartrate, Nb_3Sn, TeO_2, $KH_3(SeO_3)_2$, LaP_5O_{14} and $DyVO_4$ the transition is continuous (second order), which implies that (at least) one of the sound velocities vanishes at the transition (Lüthi & Rehwald 1981; Cummins 1982). As a consequence of the crystal anisotropy, the sound velocities depend on the direction of propagation, and thus the soft-phonon velocity does not vanish throughout the entire Brillouin zone, but only in one or several so-called soft sectors which may be one or two dimensional. For example, for the martensitic transformation in the A-15 compounds Nb_3Sn and V_3Si the transverse acoustic phonons propagating along the face diagonals of the Brillouin zone with sound velocity $c_s = \sqrt{(c_{11} - c_{12})/2\rho}$ soften, see figure 2 (Rehwald *et al.* 1972); in KCN the elastic constant c_{44} vanishes at the transition, and the soft subspaces are two dimensional (Haussühl 1973; Knorr *et al.* 1985). We remark that the actual situation may be quite complex; e.g. in the ferroelectric

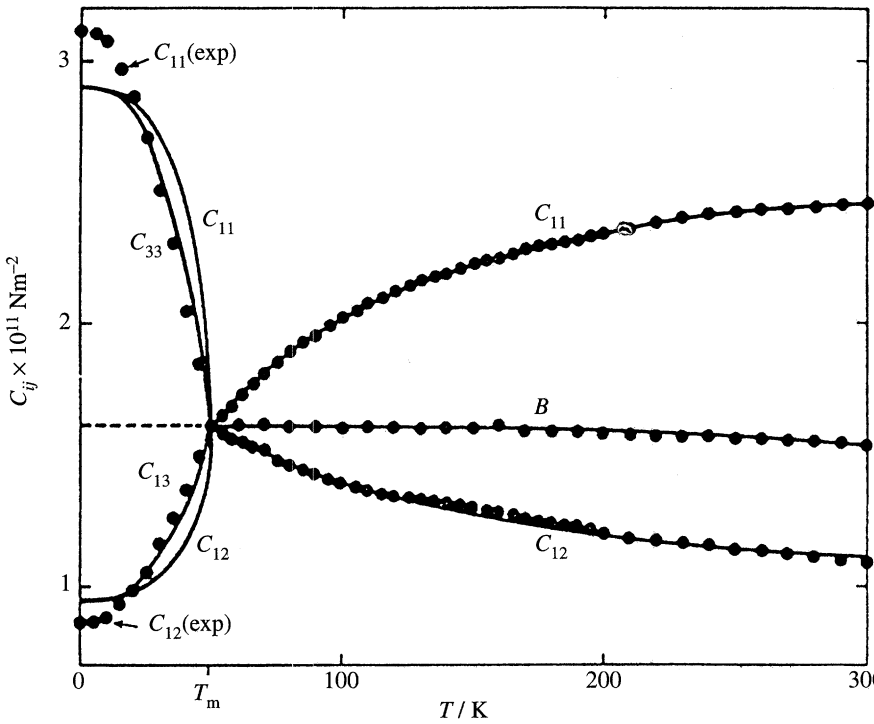

Figure 2. Elastic moduli c_{11}, c_{12}, and B of Nb_3Sn versus temperature (from Rehwald *et al.* 1972).

KDP the z-component of the electric dipole moment couples linearly to the ε_{12} shear deformation (Brody & Cummins 1974). Consequently, although caused by the ordering of hydrogen-bonding protons, the transition becomes ultimately an elastic phase transformation with vanishing shear modulus c_{66}. Similar cases, where the instability itself occurs for an optical mode that then drives the elastic transition, are LaP_5O_{14} (Fox *et al.* 1976) and h-$BaTiO_3$ (Yamaguchi *et al.* 1995), amongst others. Yet there are also cases of 'pure' elastic phase transitions, where local fluctuations render the crystal unstable, e.g. in NaOH (Bleif *et al.* 1971). The other possibility, realized in the so-called isostructural elastic phase transformations, is related to those elastic stability limits where all transverse and necessarily all longitudinal sound velocities remain finite. For instance, if the bulk modulus of an isotropic or cubic elastic medium vanishes, only the macroscopic uniform dilatation and gradient modes soften, but none of the phonons (Khmel'nitskii (1975); this kind of behaviour was observed in Ce, see Poniatovskii (1958)).

In the present brief overview, we shall focus on the theory of continuous elastic phase transitions accompanied by the softening of an acoustic phonon. We shall rely on the Ginzburg–Landau free-energy functional that was established by Cowley (1976) and Folk *et al.* (1976*a*, *b*), who also derived the Langevin equations of motion for the soft acoustic phonons (Folk *et al.* 1979). We are going to investigate the statics and soft-phonon dynamics of second-order elastic phase transitions in pure systems in § 2 and § 3, respectively; for earlier reviews, see Schwabl (1980, 1985). As a consequence of the anisotropy of the elastic system, fluctuations are reduced and the (upper) critical dimension $d_c(m) = 2 + \frac{1}{2}m$ (for the case of a m-dimensional

soft sector). This is smaller than $d_c = 4$ for a ϕ^4 model, describing either an Ising or Heisenberg magnet, or distortive structural transitions with short-range interactions. If the theory is phrased in terms of deformations, the Hamiltonian is seen to be equivalent to a spin system with long-range uniaxial dipolar interactions, which again explains why the corresponding critical dimension is lower (see § 2). The case where the elastic transition is actually driven by the linear coupling of transverse acoustic modes to a softening optical phonon will be briefly discussed in § 4.

The then surprising observation of extremely narrow central peaks in the scattering cross-section, near both distortive (Riste *et al.* 1971; Shapiro *et al.* 1972) and elastic transitions (Shirane & Axe 1971) has prompted various theoretical studies investigating the influence of lattice defects on the statics and dynamics of structural phase transformations (see, for example, Folk & Schwabl 1974; Halperin & Varma 1976; Höck & Thomas 1977; Schmidt & Schwabl 1977, 1978; Höck *et al.* 1979; Sasvári & Schwabl 1982; Weyrich & Siems 1984; Wiesen *et al.* 1987, 1988). For reviews of the experimental facts, see Müller (1979) and Fleury & Lyons (1982); some key theoretical results are collected in Bruce & Cowley (1981). Recently, these studies, which are typically concerned with distortive transformations and single-defect properties or conclusions derived by linear superposition thereof, were extended to elastic systems (Schwabl & Täuber 1991*a*), and the methods developed for distortive crystals with a truly finite concentration of impurities (Schwabl & Täuber 1991*b*) were applied to the highly anisotropic elastic structural phase transitions (Bulenda *et al.* 1996). These developments and their consequences for a possible explanation of the central-peak phenomenon are the subject of § 5. In the concluding § 6 we summarize by contrasting elastic phase transitions with distortive structural transformations, and also discuss some aspects of the related first-order martensitic transformations.

2. Static properties in pure systems

(*a*) *Ginzburg–Landau free energy functional*

In order to study elastic phase transitions, we expand the elastic free energy in terms of the strain tensor ε_{ik} (Einstein's sum convention is employed here and in the following):

$$\mathcal{F}[\{\varepsilon_{ik}\}] = \int \left[\frac{1}{2} c^{(2)}_{iklm} \varepsilon_{ik} \varepsilon_{lm} + \frac{1}{2} d^{(2)}_{iklmrs} \left(\frac{\partial}{\partial x_r} \varepsilon_{ik} \right) \left(\frac{\partial}{\partial x_s} \varepsilon_{lm} \right) + \frac{1}{3!} c^{(3)}_{iklmrs} \varepsilon_{ik} \varepsilon_{lm} \varepsilon_{rs} + \frac{1}{4!} c^{(4)}_{iklmrsuv} \varepsilon_{ik} \varepsilon_{lm} \varepsilon_{rs} \varepsilon_{uv} + \cdots \right] \mathrm{d}^3 x, \quad (2.1)$$

where the strain tensor is defined via the derivatives of the displacement field u_i,

$$\varepsilon_{ik} = \frac{1}{2} \left(\frac{\partial u_i}{\partial x_k} + \frac{\partial u_k}{\partial x_i} + \frac{\partial u_l}{\partial x_i} \frac{\partial u_l}{\partial x_k} \right), \quad (2.2)$$

and the displacement field $u_i(\boldsymbol{x})$ itself can be expanded in terms of the Fourier-space normal coordinates $Q_{\boldsymbol{k},\lambda}$ ($\lambda = 1, 2, 3$):

$$u_i(\boldsymbol{x}) = \frac{1}{\sqrt{NM}} \sum_{\boldsymbol{k},\lambda} \mathrm{e}^{\mathrm{i}\boldsymbol{k}\boldsymbol{x}} \boldsymbol{e}_i(\boldsymbol{k}, \lambda) Q_{\boldsymbol{k},\lambda}. \quad (2.3)$$

Here, $\boldsymbol{e}(\boldsymbol{k}, \lambda)$ denotes the polarization vector, M the mass and N the number of the unit cells.

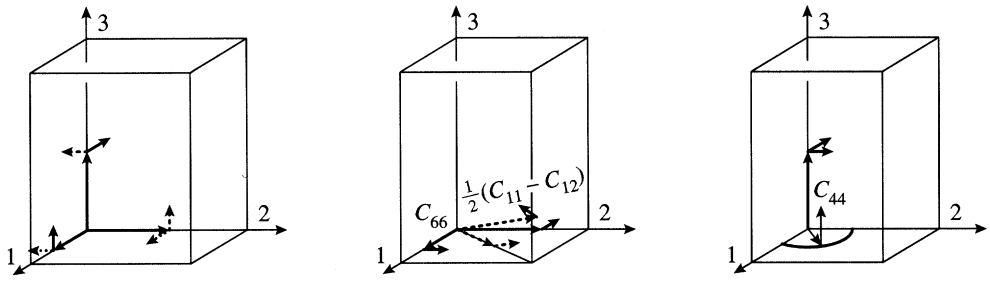

(*a*) (*b*) (*c*)

Figure 3. (*a*) Wave vectors and polarization vectors of soft transverse phonons in orthorhombic crystals; the sound velocities c_s are: $(c_{44}/\rho)^{1/2}$ (dashed), $(c_{55}/\rho)^{1/2}$ (solid), $(c_{66}/\rho)^{1/2}$ (dotted). (*b*) and (*c*) Wave vectors and polarization vectors of soft elastic modes in tetragonal crystals.

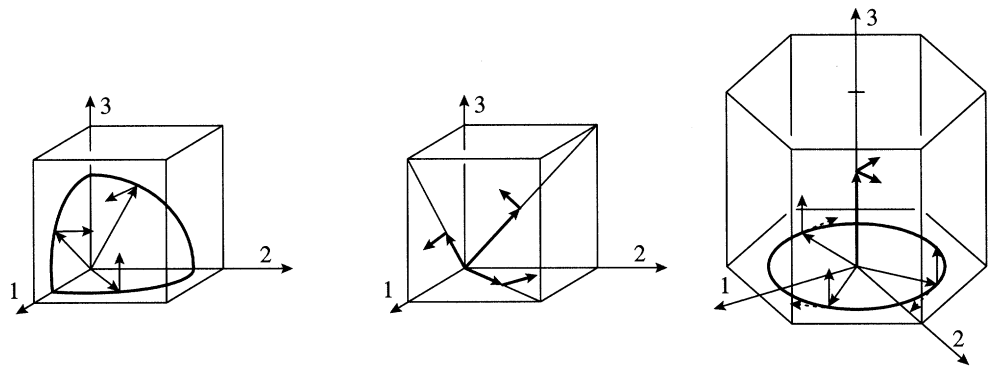

(*a*) (*b*) (*c*)

Figure 4. (*a*), (*b*) Elastic soft modes in cubic crystals, with (*a*) wave vector in one of the base planes and polarization perpendicular to it, $c_s = (c_{44}/\rho)^{1/2}$, and (*b*) wave vector in one of the face diagonals, $c_s = [(c_{11} - c_{12})/2\rho]^{1/2}$; (*c*) soft transverse phonons in the hexagonal system, with sound velocities $(c_{44}/\rho)^{1/2}$ (dashed) and $[(c_{11} - c_{12})/2\rho]^{1/2}$ (solid).

The coefficients $c^{(m)}$ in equation (2.1) are the isothermal elastic constants of order m. In addition to the terms contained in the standard expansion of the free energy in elasticity theory, we explicitly take into account contributions involving gradients of the strain tensor. Contributions of this form were introduced in so-called generalized elasticity theory, and can be derived from a lattice-dynamical model by taking the long-wavelength limit and retaining terms up to the fourth order in the wave vector k (see Krumhansl 1968; Mindlin 1968; Kunin 1968). These gradient terms are of course essential for the mathematical description of spatial fluctuations and short-range inhomogeneities.

The point-group symmetry now determines the number of independent elastic constants $c^{(2)}_{iklm}$ and, via the stability limits, the possible elastic phase transformations (see Aubry & Pick 1971; Liakos & Saunders 1982). For example, in the orthorhombic system one finds elastic phase transitions with vanishing c_{44}, c_{55} and c_{66} (we apply the Voigt notation). The corresponding wave vectors and polarization vectors are shown in figure 3*a*. In the case of higher symmetries, softening may occur in one- or two-dimensional sectors (if $c_{44} \to 0$) of Fourier space. The possible acoustic soft modes in tetragonal, cubic and hexagonal crystals are illustrated in figures 3 and 4, respectively. Since hexagonal crystals are elastically isotropic with respect to the six-

Table 1. *Elastic phase transitions*

high-temperature phase	vanishing combination of elastic constants	strain	m	third-order invariants
orthorhombic	c_{44}	ε_{23}	1	—
	c_{55}	ε_{13}	1	—
	c_{66}	ε_{12}	1	—
tetragonal II	c_{44}	ε_{23}, ε_{13}	1 + 2	—
tetragonal I	c_{44}	ε_{23}, ε_{13}	1 + 2	—
	c_{66}	ε_{12}	1	—
	$c_{11} - c_{12}$	$\varepsilon_{11} - \varepsilon_{22}$	1	—
cubic II	c_{44}	ε_{12}, ε_{13}, ε_{23}	2	$\varepsilon_{23}\varepsilon_{13}\varepsilon_{12}$
	$c_{11} - c_{12}$	e_3,e_2	1	$e_3(e_3^2 - 3e_2^2)$, $e_2(e_3^2 - 3e_2^2)$
cubic I	c_{44}	ε_{12}, ε_{13}, ε_{23}	2	$\varepsilon_{23}\varepsilon_{13}\varepsilon_{12}$
	$c_{11} - c_{12}$	e_3,e_2	1	$e_3(e_3^2 - 3e_2^2)$
hexagonal II	c_{44}	ε_{23}, ε_{13}	1 + 2	–
	$c_{66} = \frac{1}{2}(c_{11} - c_{12})$	ε_{12}, $\varepsilon_{11} - \varepsilon_{22}$	2	$(\varepsilon_{11} - \varepsilon_{22})^3$, $\varepsilon_{12}(\varepsilon_{11} - \varepsilon_{22})^2$, ε_{12}^3
hexagonal I	c_{44}	ε_{23}, ε_{13}	1 + 2	–
	$c_{66} = \frac{1}{2}(c_{11} - c_{12})$	ε_{12}, $\varepsilon_{11} - \varepsilon_{22}$	2	$(\varepsilon_{11} - \varepsilon_{22})^3$, $\varepsilon_{12}(\varepsilon_{11} - \varepsilon_{22})^2$

fold c-axis, the transverse phonons with wave vector and polarization perpendicular to the c-axis are degenerate and soften with $c_{66} = \frac{1}{2}(c_{11} - c_{12})$ going to zero.

If there are third-order invariants which lead to a cubic term in the soft phonon mode, the transition will be of first order. The third-order invariants allowed by symmetry were tabulated by Brugger (1965). For example, in cubic systems with $c_{44} \to 0$ there is a third-order term of the form $\varepsilon_{12}\varepsilon_{23}\varepsilon_{13}$; third-order terms are also present for $c_{11} - c_{12} \to 0$ in cubic and hexagonal systems. The theory described in the following is applicable, if third-order terms are either not present at all, or if they are sufficiently small in order that the ensuing first-order character of the transition will only be noticeable in the immediate vicinity of the transition temperature T_c, and the phase transformation can effectively be considered as continuous. The high-temperature phases and vanishing combination of elastic constants for the possible elastic phase transitions are listed in table 1, along with the corresponding strain components ($e_2 = (\varepsilon_{11} - \varepsilon_{22})/\sqrt{2}$, $e_3 = (\varepsilon_{11} + \varepsilon_{22} - 2\varepsilon_{33})/\sqrt{6}$), dimensionality m of the soft sectors, and the third-order invariants. For a listing of physical examples for these transformations, see Folk *et al.* (1979), Lüthi & Rehwald (1981) and Cummins (1982).

A few remarks are in place here concerning the soft-mode spectrum and the characteristic Hamiltonian or free-energy density following from expansion (2.1), as to be investigated in the following §§ 2 *b* and 3.

(i) The sound velocity vanishes only in one- or two-dimensional subspaces. In the vicinity of these directions the sound velocity is non-zero but small, and it is

important for the theory to include all phonons with wavevectors $\boldsymbol{k}$ in a finite sector around the m-dimensional soft subspace.

(ii) The gradient terms stemming from generalized elasticity theory prevent the sound frequency from vanishing throughout the entire Brillouin zone, and replace the linear by a quadratic dispersion precisely at the critical temperature T_c.

(iii) For the study of critical phenomena, we shall disregard non-critical modes and only retain the normal coordinate of the soft acoustic phonon.

(iv) We shall discard odd anharmonic terms, thus restricting the applicability of the theory to situations where these are prohibited by symmetry; this applies to orthorhombic and tetragonal crystals, or to cases where the cubic terms are sufficiently small such that the phase transition can be regarded as of nearly second order.

(*b*) *Critical statics*

We are now ready to address the static critical behaviour near elastic phase transitions. In the framework of renormalization group theory, one considers a d-dimensional crystal with an m-dimensional soft subspace (in real systems, of course, $d = 3$ and $m = 1$ or $m = 2$). Accordingly, we decompose the d-dimensional wave vector $\boldsymbol{k}$ into its m-dimensional 'soft' components $\boldsymbol{q}$ and the $(d - m)$-dimensional 'stiff' components $\boldsymbol{p}$; $\boldsymbol{k} = (\boldsymbol{q}, \boldsymbol{p})$. The Hamiltonian following from equations (2.1), (2.3) and the discussion at the end of the preceding section then reads in Fourier space (Folk *et al.* 1976*a*, *b*)

$$H[\{Q_{\boldsymbol{k}}\}] = \tfrac{1}{2} \int \mathrm{d}^d k (rp^2 + p^4 + q^2) |Q_{\boldsymbol{k}}|^2 + u \int \mathrm{d}^d k_1 \ldots \mathrm{d}^d k_4 \, v(\boldsymbol{k}_1, \ldots, \boldsymbol{k}_4) Q_{\boldsymbol{k}_1} Q_{\boldsymbol{k}_2} Q_{\boldsymbol{k}_3} Q_{\boldsymbol{k}_4}, \tag{2.4}$$

where $r \propto T - T_c$ is assumed (in the following, we shall omit the polarization indices λ). We will investigate the following two models:

$$\mathrm{I} : v(\boldsymbol{k}_1, \boldsymbol{k}_2, \boldsymbol{k}_3, \boldsymbol{k}_4) = p_1 p_2 p_3 p_4 \delta(\boldsymbol{k}_1 + \boldsymbol{k}_2 + \boldsymbol{k}_3 + \boldsymbol{k}_4), \tag{2.5}$$

$$\mathrm{II} : v(\boldsymbol{k}_1, \boldsymbol{k}_2, \boldsymbol{k}_3, \boldsymbol{k}_4) = (\boldsymbol{p}_1 \boldsymbol{p}_2)(\boldsymbol{p}_3 \boldsymbol{p}_4) \delta(\boldsymbol{k}_1 + \boldsymbol{k}_2 + \boldsymbol{k}_3 + \boldsymbol{k}_4). \tag{2.6}$$

The characteristic features of the elastic Hamiltonian (2.4) are:

(i) the anisotropy in the harmonic part, as a consequence of which fluctuations in the 'stiff' directions are suppressed; and

(ii) the wave-vector dependence of the interaction (2.5) or (2.6).

We note that the statics of model I can be mapped onto the Hamiltonian of the uniaxial dipolar magnet using the transformation $S_{\boldsymbol{k}} = pQ_{\boldsymbol{k}}$ (Cowley 1976; Folk *et al.* 1977).

Terms which are irrelevant for the critical behaviour (in the renormalization group sense) have already been omitted in the effective Hamiltonian (2.4) and interactions (2.5), (2.6). As noted previously, there is in general more than one soft sector; however, the respective interaction vanishes upon repeated application of the renormalization-group transformation. Hence we may consider the different soft sectors as independent and of the form (2.4).

The renormalization-group transformation appropriate for the anisotropic Hamiltonian (2.4) consists, as usual, of two steps.

(1) Eliminate wave vectors in the momentum shells $b^{-1} < p < 1$ for the soft, and $b^{-2+\eta/2} < q < 1$ for the stiff sector, respectively.

Table 2. *Logarithmic corrections*

model	r_χ	r_C
I	$\frac{1}{3}$	$\frac{1}{3}$
II	$\frac{4}{9}$	$\frac{1}{9}$

(2) Rescale according to $\boldsymbol{p}' = b\boldsymbol{p}$, $\boldsymbol{q}' = b^{2-\eta/2}\boldsymbol{q}$, and $Q'_{\boldsymbol{k}'} = \zeta^{-1}Q_{\boldsymbol{k}}$.

The elastic anisotropy is reflected in the different scaling for the soft and stiff sectors. This procedure yields a new effective Hamiltonian with coupling constants r' and u'. The decisive transformation is the one for the nonlinear coupling u:

$$u' = b^{4+m-2d}[u - 36u^2C(r)], \tag{2.7}$$

where $C(r)$ stems from the one-loop bubble diagram; from equation (2.7) we can immediately read off the (upper) critical dimension as a function of the dimensionality m of the soft sector (Folk *et al.* 1976*a*, *b*):

$$d_c(m) = 2 + \tfrac{1}{2}m. \tag{2.8}$$

For $d > d_c(m)$, the nonlinear coupling is irrelevant, and the system approaches a Gaussian fixed point $u^* = 0$; its critical behaviour is thus governed by the classical critical exponents. Only for $d < d_c(m)$ is a non-trivial fixed point of the renormalization-group transformation approached, and the exponents assume non-classical values.

The effective suppression of critical fluctuations now becomes evident. For one-dimensional soft sector the critical dimension is $d_c(1) = \frac{5}{2}$, and consequently elastic phase transitions in three dimensions are characterized by the classical critical exponents

$$m = 1: \quad \nu = \tfrac{1}{2}, \quad \eta = 0, \quad \gamma = 1, \quad \beta = \tfrac{1}{2}, \quad \alpha = 0, \quad \delta = 3. \tag{2.9}$$

In the case of a two-dimensional soft sector one has $d_c(2) = 3$, and one thus finds classical behaviour with logarithmic corrections in three dimensions. For instance, the static susceptibility (inverse elastic coefficient) and the specific heat are given by

$$m = 2: \quad \chi \propto \tau^{-1}|\ln\tau|^{r_\chi}, \quad C \propto |\ln\tau|^{r_C}, \tag{2.10}$$

where $\tau = |T - T_c|/T_c$. The exponents r_χ and r_C for models I and II are listed in table 2 (Folk *et al.* 1976*a*, *b*). For a second-order elastic transition in $d = 3$ with $m \geqslant 2$, the local fluctuations diverge: $\langle u^2\rangle \propto |\log\tau|$ for $m = 2$ and $\langle u^2\rangle \propto \tau^{-1/2}$ for $m = 3$; hence the Debye–Waller vanishes at T_c. It is conceivable that the actual phase transformation in such systems will be of first order, not necessarily leading to the phase indicated by the soft mode.

Elastic phase transitions with a two-dimensional soft sector occur, e.g. in KCN (Haussühl 1973), NaCN (Rowe *et al.* 1975), and s-triazene (Smith & Rae 1978; Rae 1978); in most of the cases, however, the soft sector is one dimensional.

There seems to be no isotropic elastic system that would show the onset of a shear instability, possibly as a precursor to melting. However, it is conceivable that the case $m = d$ could apply to phase transitions in disordered systems like polymer gels, which on a sufficiently large length scale can be viewed as isotropic elastic media. For isotropic elastic transformations the upper critical dimension would be $d_c(3) = \frac{7}{2}$,

and one would have non-classical behaviour in three dimensions. For elastic phase transitions of layers deposited on (preferrably amorphous) substrates, equation (2.8) predicts non-classical behaviour.

3. Dynamic properties

(*a*) *Soft acoustic phonons*

In order to derive the equations of motion for the soft acoustic phonons, we construct an effective Lagrangean from the free energy (2.1) and a kinetic term, re-expressed in terms of the displacement fields via (2.2):

$$L[\{u_i\}] = \int \frac{1}{2}\rho \left(\frac{\partial u_i(\boldsymbol{x},t)}{\partial t}\right)^2 \mathrm{d}^3x\,\mathrm{d}t - \mathcal{F}[\{u_i\}]. \tag{3.1}$$

Here, ρ denotes the mass density of the unit cell. Following nonlinear (generalized) elasticity theory the deterministic part of the equations of motion can now be obtained by applying the variational principle $\delta L[\{u_i\}]/\delta u_i(\boldsymbol{x},t) = 0$. Degrees of freedom other than the displacement field will lead to damping and noise; thus our complete Langevin-type equation of motion for the phonon normal modes becomes (Folk *et al.* 1979)

$$M\ddot{Q}_{\boldsymbol{k}} = -\frac{\delta H[\{Q_{\boldsymbol{k}}\}]}{\delta Q_{-\boldsymbol{k}}} - M\Gamma_{\boldsymbol{k}}\dot{Q}_{\boldsymbol{k}} + r_{\boldsymbol{k}}. \tag{3.2}$$

For acoustic phonons, the damping coefficient reads

$$\Gamma_{\boldsymbol{k}} = Dp^2 + \tilde{D}q^2, \tag{3.3}$$

where the damping constants D and $\tilde{D}$ for the soft and stiff sectors, respectively, are different in general. The stochastic force $r_{\boldsymbol{k}}$ results from the non-critical degrees of freedom; it has zero mean and its fluctuations are related to the damping coefficient by an Einstein relation

$$\langle r_{\boldsymbol{k}}(t) r_{\boldsymbol{k}'}(t')\rangle = 2\Gamma_{\boldsymbol{k}} k_{\mathrm{B}} T \delta(\boldsymbol{k}+\boldsymbol{k}')\delta(t-t'), \tag{3.4}$$

which guarantees that the equilibrium distribution is

$$\mathcal{P}[\{P_{\boldsymbol{k}}, Q_{\boldsymbol{k}}\}] \propto \exp\left[-\frac{1}{k_{\mathrm{B}}T}\left(\sum_{\boldsymbol{k}} \frac{|P_{\boldsymbol{k}}|^2}{2M} + H[Q_{\boldsymbol{k}}]\right)\right], \tag{3.5}$$

where $P_{\boldsymbol{k}}$ denotes the canonical momentum conjugate to $Q_{\boldsymbol{k}}$.

For $T > T_{\mathrm{c}}$, the dynamic phonon susceptibility in the mean-field approximation follows immediately from the Fourier-transformed equation of motion (3.2) with (3.3), and the harmonic part of the Hamiltonian (2.4):

$$\chi(\boldsymbol{k},\omega) = [-M\omega^2 - iM\omega(Dp^2 + \tilde{D}q^2) + rp^2 + p^4 + q^2]^{-1}. \tag{3.6}$$

The poles of $\chi(\boldsymbol{k},\omega)$ determine the phonon dispersion relation. Equation (3.6) thus shows that as $T \to T_{\mathrm{c}}$ ($r = \xi^{-2} \to 0$), the dispersion of the soft acoustic modes ($\boldsymbol{q} = 0$) turns from linear to quadratic; assuming that D stays constant, the soft mode finally becomes overdamped in the vicinity of T_{c}. The dynamical phonon correlation function $D(\boldsymbol{k},\omega)$, which is directly measured in scattering experiments as part of the dynamic structure factor $S(\boldsymbol{k},\omega)$ (see § 5 *b*), is related to the dynamic susceptibility

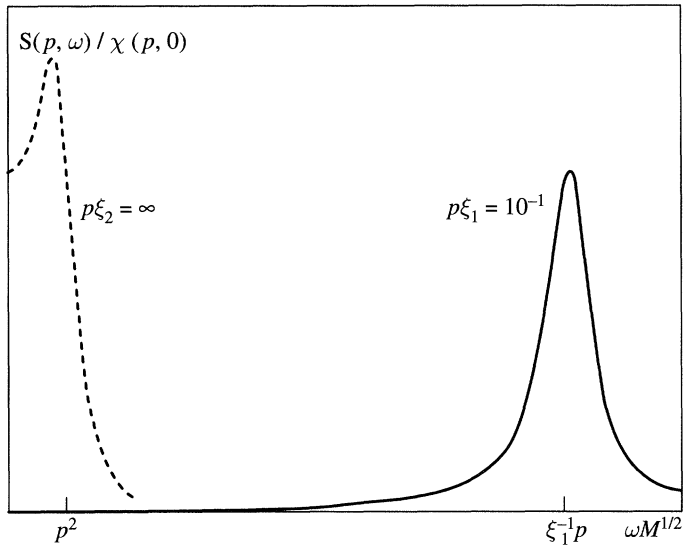

Figure 5. Dynamical correlation function for the soft acoustic phonon versus $\omega M^{1/2}$ for $q = 0$, $M^{1/2}D = 1.0$, and two values of the correlation length ξ: solid line, $p\xi_1 = 0.1$ (hydrodynamic regime); dashed line, $p\xi_2 = \infty$ (critical region).

via the (classical) fluctuation–dissipation theorem

$$D(\boldsymbol{k},\omega) = \frac{2k_{\mathrm{B}}T}{\omega}\,\mathrm{Im}\,\chi(\boldsymbol{k},\omega). \tag{3.7}$$

It is depicted in figure 5 for $\boldsymbol{q} = 0$ and $M^{1/2}D = 1.0$, both in the hydrodynamic regime ($p\xi_1 = 0.1$) and in the critical region ($p\xi_2 = \infty$).

Before turning to a more thorough analysis of the critical dynamics, we remark that, to be precise, the adiabatic elastic constants should enter the dynamical equations of motion, and not the isothermal elastic constants used in § 2. The general thermodynamic relation between adiabatic and isothermal elastic constants (of second order) is (Leibfried & Ludwig 1961)

$$c_{iklm}^{(2)\mathrm{ad}} - c_{iklm}^{(2)\mathrm{is}} = \frac{T}{C_\varepsilon}\beta_{ik}\beta_{lm}, \tag{3.8}$$

where $\beta_{ik} = (\partial\sigma_{ik}/\partial T)_\varepsilon$ is the temperature derivative of the stress tensor and C_ε is the specific heat at constant strain. In certain symmetry directions the adiabatic and isothermal sound velocities coincide; for instance, according to (3.8) $c_{11}^{\mathrm{ad}} - c_{12}^{\mathrm{ad}} = c_{11}^{\mathrm{is}} - c_{12}^{\mathrm{is}}$ (switching back to Voigt's notation). However, in a cubic crystal $c_{11}^{\mathrm{ad}} = c_{11}^{\mathrm{is}} + T\beta^2/C_\varepsilon$, and this difference might be noticeable and important when data are actually fitted over a wide temperature range.

(*b*) *Critical dynamics*

In situations where the soft mode is a propagating hydrodynamic mode, considerable information can be gained already by simply using the hydrodynamic result in conjunction with dynamical scaling. Thus one finds for the sound velocity

$$c_{\mathrm{s}} = \sqrt{c/\rho} \propto \tau^{\gamma/2} \propto \xi^{-(2-\eta)/2}, \tag{3.9}$$

where ρ is the mass density, $c \propto \tau^\gamma$ denotes an appropriate combination of elastic constants, i.e. the inverse of the static critical susceptibility, $\xi \propto \tau^{-\nu}$ is the correlation

length, and the scaling relation $\gamma = \nu(2-\eta)$ has been used. Therefore we expect for the dynamical critical exponent $z = 2 - \frac{1}{2}\eta$.

Indeed, supplementing the static rescaling operations of § 2 *b* by $\omega' = b^z\omega$, and carrying out the dynamic renormalization group program, to one-loop order the following recursion relations for the dynamical parameters M and D are found (Folk *et al.* 1979):

$$M' = b^{4-\eta-2z}M, \tag{3.10}$$

$$M'D' = b^{2-\eta-z}[MD + u^2E(D,M)\ln b]. \tag{3.11}$$

Here, the explicit form for $E(D,M)$ may be inferred from the one-loop integral, but is not important for what follows. At the Gaussian fixed point ($u^* = 0$, hence $\eta = 0$) both relations lead to

$$z = 2, \tag{3.12}$$

as expected. In the case of a one-dimensional soft sector, furthermore, the validity of the mean-field results implies that

$$c_s \propto |T - T_c|^{1/2}, \tag{3.13}$$

while the damping coefficient is temperature independent:

$$D \propto |T - T_c|^0. \tag{3.14}$$

Consequently the sound attenuation coefficient becomes

$$\alpha_s = \frac{D\omega^2}{2c_s^3} \propto |T - T_c|^{-3/2}\omega^2. \tag{3.15}$$

For $m = 1$, the dynamical susceptibility is given by the mean-field expression (3.6) (see figure 5). In the case of a two-dimensional soft sector, $r = \xi^{-2}$ has to be replaced by the inverse static susceptibility in equation (2.10). The power law (3.13) has been confirmed by many experiments; the prediction for the phonon damping was verified both by Brillouin scattering (Errandonéa 1981) and ultrasonic attenuation experiments (Garland *et al.* 1984).

Although this is of no relevance in real crystals, it is interesting to note that dynamical scaling breaks down in the hypothetical isotropic elastic system for $d < d_c$. The origin of this peculiar behaviour is the appearance of a dangerous irrelevant variable, namely $X = M^{1/2}D$, the fixed-point value of which diverges. Under these circumstances there is no definite dynamical exponent; in the immediate vicinity of T_c one finds $z = 2 + c\eta$ (as for the relaxational model A), while in the hydrodynamic region the exponent for the sound velocity is $z = 2 - \frac{1}{2}\eta$, but yet another value emerges for the damping coefficient (Folk *et al.* 1979).

4. Linear coupling of an optical to an acoustic phonon

As mentioned in the Introduction, there are frequently situations where the driving mechanism for the elastic instability is the softening of an optical phonon which couples linearly to a transverse acoustic mode, e.g. in KH_2PO_4 (KDP) and LaP_5O_{14}. Then one has to study the interaction of the acoustic and the optical modes. The ensuing coupled system can be described alternatively by modes which are linear combinations of these phonons; the actual soft mode is primarily acoustic and is governed by the characteristic anisotropic elastic Hamiltonian. Hence the resulting

critical behaviour in three dimensions is classical, even if the optical modes have their origin in short-range interactions that would by themselves allow for non-classical critical fluctuations. In KDP, there is a linear coupling of the polarization to the shear ε_{12} (Brody & Cummins 1974). In LaP_5O_{14}, a Raman-active optical phonon coupled to ε_{13} drives the transition (Fox *et al.* 1976).

A simplified Hamiltonian containing all the essential features is (Schwabl 1980)

$$H[\{q_{\boldsymbol{k}}\},\{Q_{\boldsymbol{k}}\}] = \tfrac{1}{2}\sum_{\boldsymbol{k}}[\omega_0(\boldsymbol{k})^2|q_{\boldsymbol{k}}|^2 + \omega_a(\boldsymbol{k})^2|Q_{\boldsymbol{k}}|^2 + gik_xQ_{\boldsymbol{k}}q_{-\boldsymbol{k}}] + u\sum_{\boldsymbol{k}_1}\cdots\sum_{\boldsymbol{k}_4} q_{\boldsymbol{k}_1}\cdots q_{\boldsymbol{k}_4}\Delta(\boldsymbol{k}_1+\cdots+\boldsymbol{k}_4), \tag{4.1}$$

where $\Delta(\boldsymbol{k}) = 1$ if $\boldsymbol{k}$ equals a reciprocal lattice vector and zero otherwise. $Q_{\boldsymbol{k}}$ and $q_{\boldsymbol{k}}$ are the normal coordinates of the acoustic and optical phonons, respectively, and their uncoupled dispersion relations are

$$\omega_0(\boldsymbol{k})^2 = a'(T-T_c^0)/T_c^0 + c_1k_x^2 + c_2k_y^2 + c_3k_z^2, \tag{4.2}$$

and

$$\omega_a(\boldsymbol{k})^2 = \alpha_1k_x^2 + \alpha_2k_y^2 + \alpha_3k_z^2. \tag{4.3}$$

The third and fourth term in the Hamiltonian (4.1) represent the linear coupling of the acoustic and the optical phonon, and the anharmonic interactions of the optical phonons, respectively. We note the following.

(i) The transition is driven by the optical phonon, equation (4.2). Due to the short-range interactions, the optical phonon by itself would display non-classical critical behaviour.

(ii) In KDP there are (uniaxial) dipolar forces present, and $\omega_0(\boldsymbol{k})^2$ thus contains terms $\propto k_z^2/k^2$; hence, without the coupling to the acoustic phonon, one would find logarithmic corrections to the classical exponents in three dimensions.

(iii) Equations (4.1)–(4.3) refer to the vicinity of the k_x-axis. If the acoustic phonon couples to ε_{12}, there is also a contribution $\propto ik_yQ_{\boldsymbol{k}}q_{-\boldsymbol{k}}$ in equation (4.1).

The dynamics of the coupled system are described by the stochastic equations of motion:

$$\ddot{q}_{\boldsymbol{k}} = -\frac{\delta H[\{q_{\boldsymbol{k}}\},\{Q_{\boldsymbol{k}}\}]}{\delta q_{-\boldsymbol{k}}} - \Gamma_q(\boldsymbol{k})\dot{q}_{\boldsymbol{k}} + r_{q\boldsymbol{k}}, \tag{4.4}$$

$$\ddot{Q}_{\boldsymbol{k}} = -\frac{\delta H[\{q_{\boldsymbol{k}}\},\{Q_{\boldsymbol{k}}\}]}{\delta Q_{-\boldsymbol{k}}} - \Gamma_Q(\boldsymbol{k})\dot{Q}_{\boldsymbol{k}} + r_{Q\boldsymbol{k}}. \tag{4.5}$$

The stochastic forces $r_{q\boldsymbol{k}}$ and $r_{Q\boldsymbol{k}}$ are related via Einstein relations of the form (3.4) to the damping coefficients, which have the form $\lim_{\boldsymbol{k}\to 0}\Gamma_q(\boldsymbol{k}) \neq 0$ and $\Gamma_Q(\boldsymbol{k}) = D_1k_x^2 + D_2k_y^2 + D_3k_z^2$. For small wave vectors, the modes which diagonalize the harmonic part of the Langevin equations of motion (4.4), (4.5) are given by

$$f_{1\boldsymbol{k}} = \frac{q_{\boldsymbol{k}} - \alpha(\boldsymbol{k})Q_{\boldsymbol{k}}}{\sqrt{1+|\alpha(\boldsymbol{k})|^2}}, \quad f_{2\boldsymbol{k}} = \frac{-\alpha(\boldsymbol{k})q_{\boldsymbol{k}} + Q_{\boldsymbol{k}}}{\sqrt{1+|\alpha(\boldsymbol{k})|^2}}, \tag{4.6}$$

with $\alpha(\boldsymbol{k}) = igk_x/2\omega_0(0)^2$, and the corresponding eigenfrequencies are

$$\lambda_{1/2} = \omega_{0/a}(\boldsymbol{k})^2 \pm \frac{g^2k_x^2}{4\omega_0(0)^2}. \tag{4.7}$$

For small wave vectors $\boldsymbol{k}$, the mode $f_{2\boldsymbol{k}}$ is essentially acoustic; its sound velocity in the k_x-direction, as obtained from λ_2, vanishes at the temperature

$$T_{\mathrm{c}} = T_{\mathrm{c}}^0 + \frac{T_{\mathrm{c}}^0 g^2}{4\alpha_1 a'}. \tag{4.8}$$

In terms of the new variables $f_{1/2\boldsymbol{k}}$ the Hamiltonian reads

$$H[\{f_{1/2\boldsymbol{k}}\}] = \frac{1}{2}\sum_{\boldsymbol{k}}[\lambda_1|f_{1\boldsymbol{k}}|^2 + \lambda_2|f_{2\boldsymbol{k}}|^2]$$
$$+u\sum_{\boldsymbol{k}_1}\cdots\sum_{\boldsymbol{k}_4}\frac{f_{1\boldsymbol{k}_1}+\alpha(\boldsymbol{k}_1)f_{2\boldsymbol{k}_1}}{\sqrt{1+|\alpha(\boldsymbol{k}_1)|^2}}\cdots\frac{f_{1\boldsymbol{k}_4}+\alpha(\boldsymbol{k}_4)f_{2\boldsymbol{k}_4}}{\sqrt{1+|\alpha(\boldsymbol{k}_4)|^2}}\Delta(\boldsymbol{k}_1+\cdots+\boldsymbol{k}_4). \tag{4.9}$$

It is important to realize that the terms involving $f_{2\boldsymbol{k}}$ are governed by the anisotropic Hamiltonian (2.4) with $m = 1$ and the soft direction k_x. Since λ_1 remains finite at T_{c}, $f_{1\boldsymbol{k}}$ scales as $f_{1\boldsymbol{k}} \propto b^{-2} f_{2\boldsymbol{k}}$ and is thus irrelevant for the critical behaviour. Therefore, the statics and dynamics of the phase transition at T_{c} are described by mean-field critical exponents (Schwabl 1980), as previously suggested by a self-consistency argument (Villain 1970).

Closing our discussion of pure crystals, we remark that interactions of the soft acoustic phonon with other acoustic modes have been disregarded here. For instance, terms of the form $\varepsilon_{ii} \times (\mathrm{shear})^2$ are possible, which cause a coupling of the soft transverse mode to longitudinal phonons, similar in structure to the magnetostrictive interaction in compressible magnets (Wegner 1974; Bergman & Halperin 1976). Eliminating the non-critical longitudinal fluctuations leads to additional (negative) fourth-order couplings betweeen the soft modes. One may thus anticipate that in analogy to the magnetostrictive case, the transition becomes of first order for free boundaries, and the specific-heat exponent will be positive, $\alpha > 0$. For a clamped crystal, on the other hand, the transition would remain continuous; however, clamping would interfere with the shear deformation which is characteristic of the elastic systems under consideration here.

5. Disorder effects

(*a*) *Local order parameter condensation*

Real crystals contain defects of all sorts: point disorder, dislocations, grain boundaries, etc. The more complicated the unit cell, the more likely crystal growth will lead to imperfections. Some of these defects will have a pronounced impact on the phase transition. We thus turn to the investigation of the influence of disorder on the statics and dynamics of elastic phase transitions. More specifically, we shall be interested in a certain type of inhomogeneities, which have the effect of locally changing the elastic constants, and thus softening the crystal. In this section, we shall illustrate some local features by discussing an effectively one-dimensional model with a single impurity (Schmidt & Schwabl 1977, 1978; Schwabl & Täuber 1991*a*). As a matter of fact, three-dimensional systems behave qualitatively similar, when we restrict ourselves to the soft sectors in momentum space. Understanding these single-defect properties facilitates the interpretation of the results for systems with a truly finite disorder concentration, to be addressed in § 5 *b* (Schwabl & Täuber 1991*b*; Bulenda *et al.* 1996).

The one-dimensional elastic-model free energy reads (Schmidt & Schwabl 1978)

$$\mathcal{F}[\varepsilon] = \int (\tfrac{1}{2}[a - U(x)]\varepsilon(x)^2 + \tfrac{1}{2}c\varepsilon'(x)^2 + \tfrac{1}{4}b\varepsilon(x)^4)\,\mathrm{d}x, \tag{5.1}$$

where the harmonic elastic constant vanishes at the transition temperature of the pure crystal, $a = a'(T - T_c^0)$, and the Ginzburg–Landau parameters b and c are taken to be positive constants. The disorder influence is described by the short-range defect potential $U(x)$, which can be approximated by a delta function, $U(x) = U_0\delta(x)$, if both the correlation length and the wavelengths of the characteristic fluctuations are small compared to the typical defect size, which are assumed to be comparable to the lattice constant a_0. An attractive potential with positive U_0 means that the transition temperature is locally increased. The probability distribution $\mathcal{P}[\varepsilon]$ for a configuration $\varepsilon(x)$ is given by

$$\mathcal{P}[\varepsilon] \propto \exp(-\mathcal{F}[\varepsilon]/k_\mathrm{B}T). \tag{5.2}$$

In the spirit of Ginzburg–Landau theory one determines the most probable state $\bar{\varepsilon}(x)$ from the stationarity condition $\delta\mathcal{F}[\varepsilon]/\delta\varepsilon(x) = 0$; this one-dimensional configuration then serves as an approximation for the real three-dimensional order parameter (for a review of the application of Landau theory to structural phase transitions, see, for example, Salje (1992)).

Inserting (5.2) yields the nonlinear second-order differential equation

$$c\varepsilon(x)'' = [a - U(x)]\varepsilon(x) + b\varepsilon(x)^3 \tag{5.3}$$

for the stationary state, which of course always has the constant solution $\bar{\varepsilon}_0 = 0$ (note, however, that the constant solutions for $T < T_c^0$, $\bar{\varepsilon}_\pm = \pm\sqrt{|a|/b}$ describing the two possible orientations of the ordered state, are no longer allowed if $U_0 \neq 0$). Due to the defect influence, this homogeneous state may become unstable at a certain temperature $T_c^\mathrm{l} > T_c^0$, and instead a localized order parameter condensate (cluster) near the defect may form (Schmidt & Schwabl 1978); T_c^l is called local transition temperature, although it does not define a proper phase transition. Linear stability analysis shows that in the one-dimensional model local condensation occurs at

$$T_c^\mathrm{l} = T_c^0 + \frac{U_0^2}{4a'c}, \tag{5.4}$$

for any positive defect strength U_0. For $T < T_c^\mathrm{l}$ one finds the following stable cluster configurations (see figure 6) in the interval $T_c^0 \leqslant T \leqslant T_c^\mathrm{l}$,

$$\bar{\varepsilon}_>(x) = \frac{\pm\sqrt{2a/b}}{\sinh(|x|/\xi_> + \rho_>)}, \tag{5.5}$$

where $\xi_> = \sqrt{c/a}$ and $\rho_> = \operatorname{arcoth}(U_0/2\sqrt{ac})$; and in the temperature range $T < T_c^0$

$$\bar{\varepsilon}_<(x) = \pm\sqrt{|a|/b}\coth(|x|/\xi_< + \rho_<), \tag{5.6}$$

with $\xi_< = \sqrt{2c/|a|}$ and $\rho_< = \frac{1}{2}\operatorname{arsinh}(\sqrt{8|a|c}/U_0)$. Note that the widths of both configurations are given by the correlation lengths of the pure system $\xi_>$ and $\xi_<$, respectively. We remark that in $d > 1$ dimensions, in general a certain minimum disorder potential strength must be exceeded for local condensation to occur (Schmidt & Schwabl 1977; Schwabl & Täuber 1991*b*); but the ensuing order parameter cluster still decays exponentially $\propto \mathrm{e}^{-r/\xi}$ for large $r \gg \xi$.

PHILOSOPHICAL TRANSACTIONS OF THE ROYAL SOCIETY A MATHEMATICAL, PHYSICAL & ENGINEERING SCIENCES

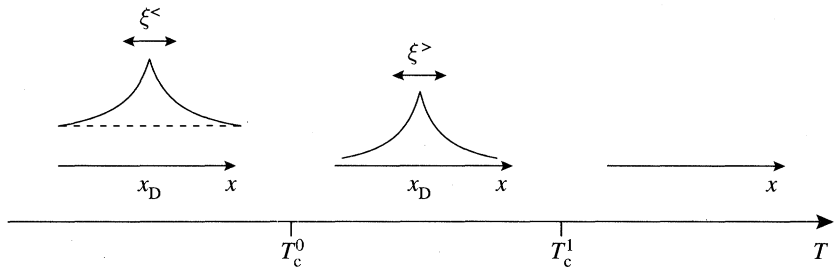

Figure 6. Local condensation: sketch of the order parameter profiles in a single-defect system in the temperature ranges $T < T_c^0$, $T_c^0 \leqslant T \leqslant T_c^1$, and $T > T_c^1$, respectively.

One can now look for traces of the local order parameter condensation in the spectrum of the soft phonons. The one-dimensional model (5.1) applies for both distortive and elastic transitions, and hence the static single-defect properties are completely analogous. However, their respective dynamics are very different: in the case of distortive transitions, one may obtain the spectrum of the optical phonons for $T \geqslant T_c^1$ by linearizing equation (5.3) about the stationary solution $\bar{\varepsilon}_0 = 0$; as a result of the 'attractive' defect, one additional localized mode emerges below the continuum of propagating scattering states, and its frequency vanishes precisely at the local transition temperature (5.4). This softening of a localized defect excitation can thus be viewed as a dynamical precursor for the local condensation in distortive systems (Schmidt & Schwabl 1978).

Similar localized acoustic phonon modes have been hypothesized for elastic systems, namely for the related first-order martensitic transformations (Clapp 1973, 1979, 1981). When supplemented with a dynamical equation of the form (3.2), the simplified one-dimensional model (5.1) permits an analytic solution. Linearizing the equation of motion yields a fourth-order differential equation for the soft acoustic modes, the eigenstates of which are linear combinations of propogating ($\propto \mathrm{e}^{\pm \mathrm{i}kx}$) and exponentially localized ($\propto \exp(\pm\sqrt{\xi_>^{-2} + k^2}x)$) contributions. Employing the appropriate boundary conditions for the delta-function defect, one finds that there appears no additional mode in the elastic system; any dispersion-free localized mode would be unstable towards decay into continuum states. Instead, each of the propagating modes contains a localized vibrational contribution in the defect vicinity, which for the long-wavelength modes ($k \to 0$) condenses as $T \to T_c^1$, in the sense that an incoming phonon is not transmitted through the defect region, but the local order parameter condensate is formed (Schwabl & Täuber 1991*a*). Accordingly, the delay time of an incoming wave packet diverges $\propto (T - T_c^1)^{-1}$ as T_c^1 is approached, as does the relaxation time of a stress-induced cluster above the local transition.

(*b*) *Disorder-induced phase transition and central peak*

By appropriately averaging the single-defect solutions, one may already infer some properties of a crystal with $N_D \gg 1$ defects, the concentration $n_D = N_D/N$ of which is to remain finite in the thermodynamic limit (Schwabl & Täuber 1991*a*). Instead, we proceed to study such a system in d space dimensions using a more direct approach (Schwabl & Täuber 1991*b*; Bulenda *et al.* 1996). It is now more convenient to use a lattice representation, and we therefore define the short-range quenched impurity potential produced by N_D point defects, located on the randomly selected lattice

sites i_{D} as

$$\phi_{ij} = \lambda \sum_{i_{\mathrm{D}}=1}^{N_{\mathrm{D}}} \delta_{i,i_{\mathrm{D}}} \delta_{ij}, \tag{5.7}$$

with Fourier transform (note that the system is not translation invariant)

$$\phi_{\boldsymbol{k}\boldsymbol{k}'} = \frac{1}{N} \sum_{i,j=1}^{N} \phi_{ij} \mathrm{e}^{-\mathrm{i}(\boldsymbol{k}\boldsymbol{x}_i - \boldsymbol{k}'\boldsymbol{x}_j)}. \tag{5.8}$$

As in the previous section, we require that $\lambda = U_0/a_0^d > 0$ such that the defects locally enhance the transition temperature. One can then write the harmonic part of the elastic Hamiltonian (2.4), supplemented by the disorder potential, as

$$H[\{Q_{\boldsymbol{k}}\}] = \int \mathrm{d}^d k \int \mathrm{d}^d k' \, \tfrac{1}{2}[(ap^2 + \alpha q^2 + cp^4)\delta_{\boldsymbol{k}\boldsymbol{k}'} - (\boldsymbol{k}\boldsymbol{k}')\phi_{\boldsymbol{k}\boldsymbol{k}'}] Q_{\boldsymbol{k}} Q_{-\boldsymbol{k}'} + \mathcal{O}(Q_{\boldsymbol{k}}^4), \tag{5.9}$$

where $a = a'(T - T_{\mathrm{c}}^0)$, and $\alpha, b > 0$ are constants. In addition to the thermal average, for this system with random quenched disorder each physical quantity has to be averaged over all possible defect configurations; the formal definition of this quenched disorder average is

$$\langle\langle \cdots \rangle\rangle = \prod_{j=1}^{N_{\mathrm{D}}} \left[\frac{1}{N} \sum_{i_{\mathrm{D}_j}=1}^{N} \right] \cdots. \tag{5.10}$$

The soft-phonon dynamics is given by the Langevin equation (3.2), with equation (3.3) and (3.4). In the pure system, the ('free') phonon propagator reads (see equation (3.6))

$$\chi_0(\boldsymbol{k}, \omega)^{-1} = -M\omega^2 - \mathrm{i}M\omega(Dp^2 + \tilde{D}q^2) + ap^2 + \alpha q^2 + cp^4. \tag{5.11}$$

Introducing an external field $h_{\boldsymbol{k}}$ in the equation of motion, inverting its Fourier transform, taking the thermal average, and differentiating it with respect to $h_{\boldsymbol{k}}$, one arrives at the following recursion relation for the 'full' dynamic response function in the high-temperature phase,

$$\chi(\boldsymbol{k}, \boldsymbol{k}', \omega) = \chi_0(\boldsymbol{k}, \omega)\delta_{\boldsymbol{k}\boldsymbol{k}'} + \chi_0(\boldsymbol{k}, \omega) \sum_{\boldsymbol{k}''} (\boldsymbol{k}\boldsymbol{k}'') \phi_{\boldsymbol{k}\boldsymbol{k}''} \chi(\boldsymbol{k}'', \boldsymbol{k}', \omega). \tag{5.12}$$

Systematical iteration of equation (5.12), and then performing the configurational average (5.10) finally yields the translationally invariant response function $\chi(\boldsymbol{k}, \omega)$ (for a diagrammatic representation, see Schwabl & Täuber 1991*b*). Collecting all contributions that are linear in the defect concentration n_{D} (single-site approximation), one eventually finds (Bulenda *et al.* 1996)

$$\chi(\boldsymbol{k}, \omega)^{-1} = \chi_0(\boldsymbol{k}, \omega)^{-1} - \frac{\lambda n_{\mathrm{D}}(p^2 + q^2)}{1 - \lambda(a_0/2\pi)^d \displaystyle\int^{\Lambda} (p^2 + q^2)\chi_0(\boldsymbol{k}, \omega) \, \mathrm{d}^m p \, \mathrm{d}^{d-m} q}, \tag{5.13}$$

where the momentum cut-off $\Lambda \approx 2\pi/a_0$ has been introduced.

The result (5.13) implies that as a consequence of the coupling to the softening defects, the entire system may become unstable towards a new low-temperature phase with finite average order parameter at a certain temperature $T_{\mathrm{c}}(n_{\mathrm{D}})$, which is

PHILOSOPHICAL TRANSACTIONS OF THE ROYAL SOCIETY A MATHEMATICAL, PHYSICAL & ENGINEERING SCIENCES

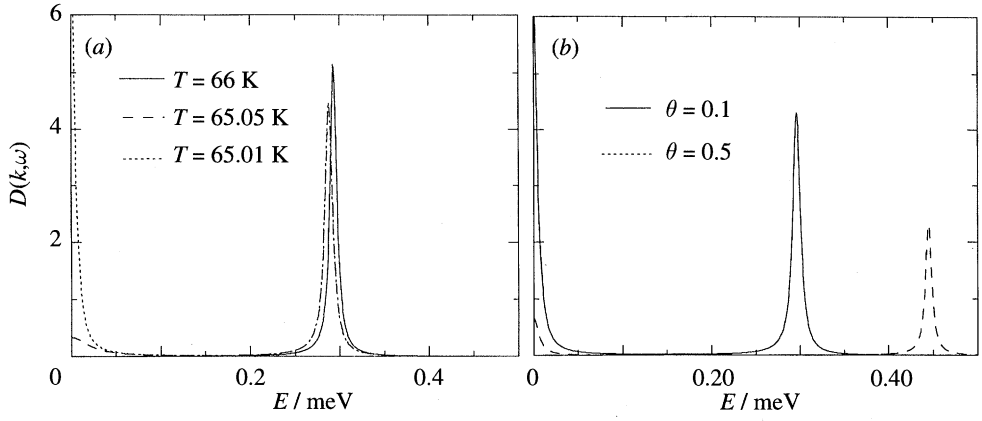

Figure 7. Dynamical phonon correlation function (with model parameters appropriate for Nb_3Sn): (*a*) for different temperatures T and fixed angle $\theta = 0$, and (*b*) for fixed temperature $T = 65.01\,\mathrm{K}$ with different angles θ between external wave vector and soft sector ($T_c(n_D) = 65\,\mathrm{K}$).

to be determined from the condition

$$\lim_{k\to 0}[k^{-2}\chi(\boldsymbol{k}, \omega = 0)^{-1}] = 0. \tag{5.14}$$

As for distortive transitions (Schwabl & Täuber 1991*b*), for $d > 1$ a certain minimum defect strength is required for this instability to occur, and $T_c(n_D)$ is bounded below by the local transition temperature T_c^l of § 5 *a*, which can be considerably higher than T_c^0, the transition temperature of the pure system.

In the response and correlation functions, the singularity at $T_c(n_D)$ appears as a dynamical central peak. In view of the single-defect properties of the previous section, one may understand this peak as stemming from overlapping localized vibrations at the point defects which 'condense' at $T_c(n_D)$, thereby forming a spatially inhomogeneous order parameter configuration. In figure 7 the dynamical correlation function (3.7) is depicted for the case of an elastic system with a one-dimensional soft sector; the numerical values used for the Ginzburg–Landau parameters there are appropriate for Nb_3Sn ($T_c^0 = 45\,\mathrm{K}$), and the defect strength λ was adjusted arbitrarily in order that $T_c(n_D) = 65\,\mathrm{K}$ (Bulenda *et al.* 1996). As $T \to T_c(n_D)$ from above, the soft phonon peak at finite energy is shifted to lower frequencies, and a very sharp and distinctive dynamical central peak emerges (figure 7*a*). Figure 7*b* shows the dependence on the angle θ between the external wave vector $\boldsymbol{k}$ and the soft sector; both graphs demonstrate that the dynamical central peak is confined to temperatures very close to the defect-induced phase transition at $T_c(n_D)$, and to wave vectors within the soft sector, reflecting the fact that wave vectors in the stiff directions do not probe the critical properties of the crystal.

The properties of the ensuing inhomogeneous low-temperature phase may be studied using a self-consistent mean-field approach (Schwabl & Täuber 1991*b*; Bulenda *et al.* 1996). The starting point is the following discrete version of the nonlinear Ginzburg–Landau free energy for a single-component order parameter ε_i in d dimensions (cf. equations (2.1) and (5.1)),

$$\mathcal{F}[\varepsilon_i] = \tfrac{1}{2}\sum_{i,j=1}^{N}\varepsilon_i G_{0ij}^{-1}\varepsilon_j - \tfrac{1}{2}\lambda\sum_{i=1}^{N}\sum_{i_D=1}^{N_D}\varepsilon_i^2\delta_{i,i_D} + \tfrac{1}{4}b\sum_{i=1}^{N}\varepsilon_i^4 - \sum_{i=1}^{N}h_i\varepsilon_i, \tag{5.15}$$

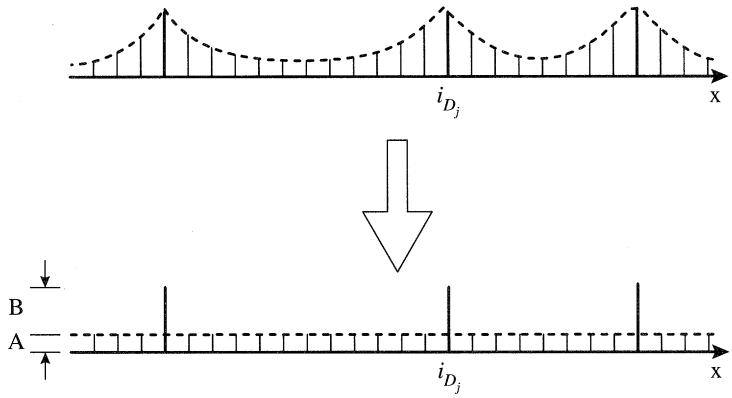

Figure 8. Schematic illustration of the order parameter configuration according to the approximations used here.

where a stress term $\propto h_i$ has been introduced, and the static propagator G_{0ij}^{-1} is defined by its Fourier transform

$$G_0(\boldsymbol{k})^{-1} = \frac{ap^2 + \alpha q^2 + cp^4}{k^2}. \tag{5.16}$$

In the framework of the Ginzburg–Landau approximation, i.e. neglecting order parameter fluctuations, the stationarity condition becomes (with constant external stress $h_i = h$)

$$\sum_j G_{0\,ij}^{-1}\varepsilon_j - \lambda \sum_{i_D} \varepsilon_i \delta_{i,i_D} + b\varepsilon_i^3 = h. \tag{5.17}$$

The solution of equation (5.17), with its combined nonlinearity and randomness, in general poses a formidable problem. Therefore an additional approximation is employed, namely the following ansatz for the thermodynamical average $\bar{\varepsilon}_i$ of the order parameter is used,

$$\bar{\varepsilon}_i = A + B \sum_{i_D} \delta_{i,i_D}, \tag{5.18}$$

i.e. the order parameter at each lattice point i is assumed to be the sum of a homogeneous background A and an additional contribution B, if there is a defect at site i, thus enhancing the total value of the order parameter to $A + B$ (see figure 8). Thus we use the approximation that at all defect sites the order parameter points in the same direction, and in addition neglect the spatial variation of the order parameter near the defects. This seemingly rather crude ansatz already contains the possible relevant modifications which can be caused by the impurities, namely (i) an enhancement of the spatially averaged order parameter (corresponding to the parameter A), and (ii) the ensuing 'screening' of the defect potential (described by B).

Inserting ansatz (5.18) into stationarity equation (5.17) yields

$$\bar{\varepsilon}_{\boldsymbol{k}} = h\delta_{\boldsymbol{k},\boldsymbol{0}}\tilde{G}_0(\boldsymbol{k}) + \tilde{G}_0(\boldsymbol{k}) \sum_{\boldsymbol{k}'} \tilde{\phi}_{\boldsymbol{k}\boldsymbol{k}'}\bar{\varepsilon}_{\boldsymbol{k}'}, \tag{5.19}$$

where a renormalized propagator

$$\tilde{G}_0(\boldsymbol{k})^{-1} = G_0(\boldsymbol{k})^{-1} + bA^2 \tag{5.20}$$

and screened defect potential $\tilde{\phi}_{\boldsymbol{k}\boldsymbol{k}'}$ with weakened strength

$$\tilde{\lambda} = \lambda - b[(A+B)^2 - A^2] \tag{5.21}$$

have been introduced. As equation (5.12) for the dynamics in the high-temperature phase, the recursion relation (5.19) can be iterated and then the quenched disorder average performed, with the single-site approximation result

$$\langle\langle\bar{\varepsilon}\rangle\rangle \left[a + bA^2 - \frac{\tilde{\lambda} n_{\mathrm{D}}}{1 - \tilde{\lambda}(a_0/2\pi)^d \int_0^{\Lambda} \tilde{G}_0(\boldsymbol{k})\, \mathrm{d}^d k} \right] = h. \tag{5.22}$$

On the other hand, immediate averaging of equation (5.17) gives

$$(a + bA^2)(A + n_{\mathrm{D}} B) - \tilde{\lambda} n_{\mathrm{D}}(A + B) = h. \tag{5.23}$$

Equations (5.22) and (5.23) constitute two coupled nonlinear equations that uniquely determine the mean order parameter; assuringly, for $h \to 0$ they yield non-zero self-consistent solutions for $\langle\langle\varepsilon\rangle\rangle$ precisely when $T < T_{\mathrm{c}}(n_{\mathrm{D}})$, the transition point determined from the instability of the high-temperature phase. Figure 9 shows that the order parameter of the disordered crystal as function of T looks similar to the corresponding curve for the pure system, with the singularity at T_{c}^0 being smeared out by the defects (in the graph, the reduced temperature $t = (T - T_{\mathrm{c}}^0)/T_{\mathrm{c}}^0$ is used). The order parameter sets in continuously at $T_{\mathrm{c}}(n_{\mathrm{D}})$, with the usual mean-field exponent $\beta = \frac{1}{2}$, remains minute in the range $T_{\mathrm{c}}(n_{\mathrm{D}}) > T > T_{\mathrm{c}}^0$, and starts to grow to larger values only near T_{c}^0. Thus the transition temperature of the pure system remains an important parameter even in the perturbed system, although the true phase transition takes place at $T_{\mathrm{c}}(n_{\mathrm{D}})$, which, however, may in fact be hardly noticeable in experiments. Again, the results for a three-dimensional system with one one-dimensional soft sector are depicted, but the qualitative features are essentially the same in the cases of a two- (or even three-) dimensional soft sector.

Inserting the self-consistent solutions for the mean order parameter as function of temperature into the free energy (5.15), the specific heat in the Landau approximation is readily determined by taking the derivatives with respect to T, $C_v = -T(\partial^2 \mathcal{F}[\bar{\varepsilon}]/\partial T^2)_V$ (see figure 10). Obviously, the discontinuity at T_{c}^0 has been smeared out, in place of which a tiny jump emerges at $T_{\mathrm{c}}(n_{\mathrm{D}})$. Note that there is a very distinct maximum of the specific heat near T_{c}^0, while the extremely minute jump at $T_{\mathrm{c}}(n_{\mathrm{D}})$ might not be experimentally detectable at all.

The dynamical phonon response and correlation functions may similarly be calculated following the above procedures; using ansatz (5.18) leads to a recursion relation precisely of the form (5.12), where modified parameters

$$a \to a + 3bA^2, \quad \alpha \to \alpha + 3bA^2, \quad \lambda \to \lambda - 3bB(2A + B) \tag{5.24}$$

are to be inserted. One finds that the dynamical central peak in the phonon correlation function rapidly disappears as the temperature is lowered below $T_{\mathrm{c}}(n_{\mathrm{D}})$.

However, there is a very interesting additional static contribution to the dynamic structure factor, caused by the defect-induced spatial inhomogeneity of the order parameter. The dynamic structure factor, as measured in scattering experiments, is defined as

$$S(\boldsymbol{k}, \omega) = \int \mathrm{e}^{\mathrm{i}\omega t} \left\langle \frac{1}{N} \sum_{i,j=1}^{N} \mathrm{e}^{-\mathrm{i}\boldsymbol{k}[\boldsymbol{a}_i + \boldsymbol{u}_i(t)]} \mathrm{e}^{\mathrm{i}\boldsymbol{k}[\boldsymbol{a}_j + \boldsymbol{u}_j(0)]} \right\rangle \mathrm{d}t, \tag{5.25}$$

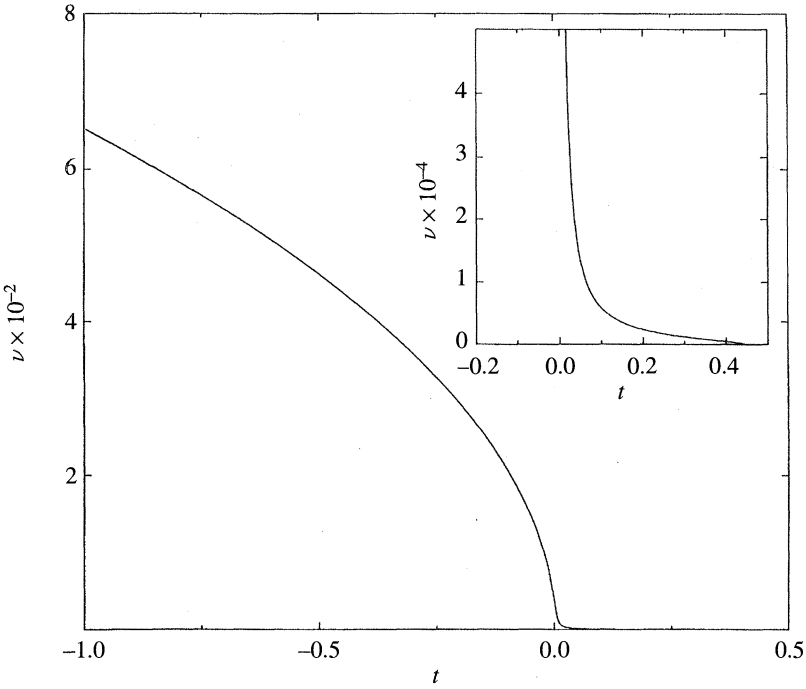

Figure 9. Average order parameter $\langle\langle\bar{\varepsilon}\rangle\rangle$ versus reduced temperature $t = (T - T_c^0)/T_c^0$: (parameters appropriate for Nb_3Sn); the region near $t_c(n_D) = 0.444$ is magnified in the inset.

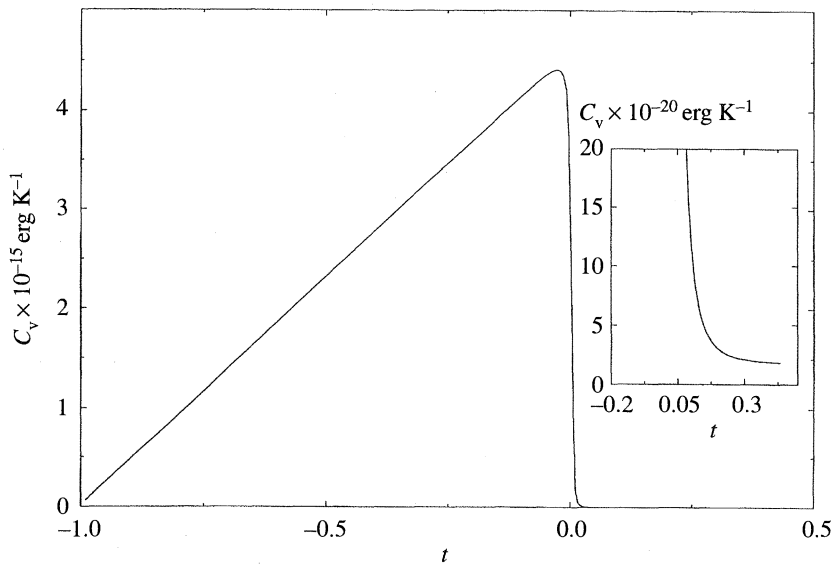

Figure 10. Specific heat C_v versus reduced temperature t: (parameters appropriate for Nb_3Sn) the region near $t_c(n_D) = 0.444$, where the discontinuity occurs, is magnified in the inset.

where $\boldsymbol{a}_i$ denote the Bravais lattice sites, and $\boldsymbol{u}_i$ the displacements from these equilibrium positions. In order to evaluate $\langle\langle S(\boldsymbol{k},\omega)\rangle\rangle$, we perform a cumulant expansion for the combined thermal and configurational averages of the exponentials in (5.25)

and expand to second order, decomposing the displacement fields $\boldsymbol{u}_i(t)$ into a static part $\bar{\boldsymbol{u}}_i$ and a fluctuating contribution $\tilde{\boldsymbol{u}}_i(t)$. Eventually one arrives at (Schwabl & Täuber 1991*b*; Bulenda *et al.* 1996)

$$\langle\langle S(\boldsymbol{k},\omega)\rangle\rangle = 2\pi\delta(\omega)\left[N\sum_{\boldsymbol{g}}\delta_{\boldsymbol{k},\boldsymbol{g}} + \sum_{\alpha\beta} k^\alpha k^\beta \langle\langle S_{\mathrm{c}}^{\alpha\beta}(\boldsymbol{k})\rangle\rangle\right]\mathrm{e}^{-2W} + \left[\sum_{\alpha\beta} k^\alpha k^\beta D^{\alpha\beta}(\boldsymbol{k},\omega)\right]\mathrm{e}^{-2W}, \tag{5.26}$$

where the first term represents the elastic Bragg scattering peaks occuring at the reciprocal lattice vectors $\boldsymbol{g}$, W is the Debye–Waller factor, and

$$S_{\mathrm{c}}^{\alpha\beta}(\boldsymbol{k}) = \frac{1}{N}\sum_{i,j}\mathrm{e}^{-\mathrm{i}\boldsymbol{k}(\boldsymbol{a}_i-\boldsymbol{a}_j)}(\bar{u}_i^\alpha\bar{u}_j^\beta - \langle\langle\bar{u}^\alpha\rangle\rangle\langle\langle\bar{u}^\beta\rangle\rangle) \tag{5.27}$$

yields an additional static contribution to the structure factor arising from elastic scattering from random variations of the local order parameter (Huang scattering); finally, $D^{\alpha\beta}(\boldsymbol{k},\omega)$ is the dynamical phonon correlation function (3.7) and (5.13), discussed before, describing inelastic scattering processes.

In the framework of the above self-consistent mean-field theory and single-site approximation, the Huang scattering amplitude is readily obtained observing that $\bar{\epsilon}_{\boldsymbol{k}} = \boldsymbol{k}\bar{\boldsymbol{u}}_{\boldsymbol{k}}$, and using iterations of equation (5.19), with the result

$$k^2 S_{\mathrm{c}}^{\alpha\beta}(\boldsymbol{k}) = \frac{n_{\mathrm{D}}\tilde{\lambda}^2\langle\langle\bar{\varepsilon}\rangle\rangle^2 k^\alpha k^\beta \tilde{G}_0(\boldsymbol{k})^2}{\left[1-\tilde{\lambda}(a_0/2\pi)^d\int^{\Lambda}\tilde{G}_0(\mathbf{k}')\,\mathrm{d}^d k'\right]^2} = (a+bA^2)^2\frac{\langle\langle\bar{\varepsilon}\rangle\rangle^2}{n_{\mathrm{D}}}k^\alpha k^\beta\tilde{G}_0(\boldsymbol{k})^2, \tag{5.28}$$

where in the final step the condition (5.22) (for $h \to 0$) was used. Note that the renormalized static susceptibility, which determines this additional elastic scattering amplitude, does not diverge at T_{c}^0; furthermore, this static central peak is characterized by a finite width in momentum space, $\gamma = \sqrt{(a+bA^2)/c}$ (if $\boldsymbol{k}$ lies in the soft sector), which vanishes at the defect-induced transition temperature $T_{\mathrm{c}}(n_{\mathrm{D}})$. Figure 11 depicts the Huang scattering amplitude (5.28) as a function of temperature for different wave vectors $\boldsymbol{k} = \boldsymbol{p}$ in the soft sector. The static central peak emerges at $T_{\mathrm{c}}(n_{\mathrm{D}})$, and grows to considerable intensity near T_{c}^0, but becomes less prominent and widens in $\boldsymbol{k}$ space for $T < T_{\mathrm{c}}^0$, as the order parameter slowly approaches the spatially homogeneous configuration of the undisturbed system. The dynamical central peak found in the phonon correlation function near $T_{\mathrm{c}}(n_{\mathrm{D}})$ may be viewed as its dynamical precursor in the critical region, as well as the static one due to the new Bragg peaks which of course persist through the entire low-temperature phase.

At this point we have to comment on the applicability of our mean-field approach. Although we have explained in § 2 that critical fluctuations only play a minor role for elastic phase transitions, the situation here is somewhat different, for we now have to worry about local fluctuations in the orientations of the disorder-induced order parameter clusters (5.5), which were entirely neglected in the previous treatment. The mean-field approximation suggests that as soon as these local condensates form at $T_{\mathrm{c}}(n_{\mathrm{D}}) \approx T_{\mathrm{c}}^{\mathrm{l}}$, a coherent order parameter with non-zero mean emerges, independent of space dimension d. More realistically, one would expect that while at $T_{\mathrm{c}}^{\mathrm{l}}$ local

PHILOSOPHICAL TRANSACTIONS OF THE ROYAL SOCIETY A MATHEMATICAL, PHYSICAL & ENGINEERING SCIENCES

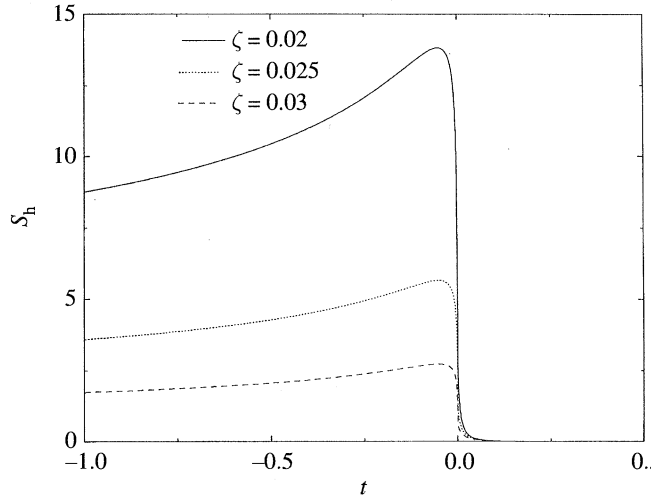

Figure 11. Huang scattering intensity $S_c(\boldsymbol{k})$ versus reduced temperature t for different wave numbers $k = \zeta 2^{3/2}\pi/a_0$; the wave vector $\boldsymbol{k}$ lies in the soft sector.

condensation at the defects takes place, yet the orientations of the different clusters still fluctuate considerably, and they possibly form a true new ground state only at a lower temperature T_{ord}. A crude estimate of this true ordering temperature is obtained by the criterion that the correlation length should at least be of the order of the mean defect separation $\propto n_{\mathrm{D}}^{-1/d}$ for collective behaviour of the condensates to occur. A more refined argument considers the different cluster orientations as effectively Ising-like degrees of freedom, and determines $T_{\mathrm{ord}} = J/k_{\mathrm{B}}$, where J is the free-energy difference between configurations with parallel and opposite cluster orientations (Bulenda *et al.* 1996). In $d = 3$ dimensions, the resulting 'true' phase transition temperature is considerably lower than $T_{\mathrm{c}}(n_{\mathrm{D}})$ for identical disorder concentration, but may still be well above T_{c}^0; thus, at least for $T \leqslant T_{\mathrm{ord}}$ a spatially inhomogeneous order parameter appears, which produces a static central peak with finite width in momentum space for temperatures above the transition temperature of the pure system, where the average order parameter is still very small. In addition, the time scale of the cluster orientation fluctuations will diverge $\propto (T - T_{\mathrm{ord}})^{-1}$ upon approaching T_{ord}, which in experiment would eventually render these indistinguishable from static inhomogeneities. Qualitatively, at least, the situation will then appear as shown in figures 9–11, with $T_{\mathrm{c}}(n_{\mathrm{D}})$ replaced by T_{ord} (or even a somewhat higher temperature, depending on the experimental frequency resolution).

(c) *Disorder and critical properties*

Another important issue is the question if disorder may change the critical properties near elastic phase transitions, i.e. if the static and dynamical critical exponents are determined by a new renormalization-group fixed point. We briefly discuss the two relevant cases of (i) random fields, and (ii) random-T_{c} disorder, and their possible influence in the critical region very close to T_{c} (Morgenstern 1988).

Quenched random fields couple linearly to the order parameter, and are taken to have vanishing average $\langle h_{\boldsymbol{k}} \rangle$ and second moment

$$\langle h_{\boldsymbol{k}} h_{\mathbf{k}'} \rangle = \Delta k^{-\Theta} \delta(\boldsymbol{k} - \mathbf{k}'), \tag{5.29}$$

where $\Theta = 0$ for short-range disorder correlation, while $0 < \Theta < m$ for long-range

correlated defects. Analysing the renormalization-group recursion relations, one finds that these random fields may alter the pure result for the (upper) critical dimension (2.8) to

$$d_c(m) = 3 + \tfrac{1}{2}m + \tfrac{1}{2}\Theta, \tag{5.30}$$

where m denotes the dimension of the soft sector (Morgenstern 1988). One therefore expects non-classical critical exponents in three-dimensional crystals undergoing an elastic phase transformation under the influence of random strain fields.

For disorder coupling quadratically to the order parameter, i.e. of the random-T_c type, on the other hand, a variant of the Harris criterion may be formulated. Again introducing possible long-range correlations

$$\langle \delta r_{\boldsymbol{k}} \delta r_{\boldsymbol{k}'} \rangle = W k^{-\Theta} \delta(\boldsymbol{k} - \boldsymbol{k}'), \tag{5.31}$$

one finds that the second-order elastic phase transitions remains to be governed by the pure critical exponents, provided that

$$\alpha + \nu\Theta < 0, \tag{5.32}$$

where α and ν denote the specific heat and correlation length critical exponents, respectively (Morgenstern 1988). For the case of point defects ($\Theta = 0$) this means that new randomness-induced critical exponents emerge if $\alpha > 0$, which is thus only possible for Ising-type systems.

6. Summary and comparison with related materials

In conclusion, we summarize the above results and contrast them with related displacive structural phase transformations, namely (1) second-order distortive transitions, and (2) first-order martensitic transitions.

For second-order distortive structural phase transitions, the order parameter is the displacement field corresponding to a soft optical phonon, while for elastic transformations the relevant collective variable is a certain combination of strain tensor components, and the soft mode is typically a transverse acoustic phonon. This means that while in the distortive case at T_c one of the optical modes softens at a specific $\boldsymbol{k}$ vector, an elastic instability implies the vanishing of the sound velocity along the soft sector in the Brillouin zone. As we have seen in § 2, as a consequence of the ensuing strong anisotropy critical fluctuations are suppressed, and continuous elastic phase transitions in three dimensions are governed by the classical critical exponents (for a one-dimensional soft sector) with at most logarithmic corrections to the scaling functions (for a two-dimensional soft sector). For distortive structural transitions, on the other hand, critical fluctuations can be quite prominent and have important effects on the values of the critical exponents (see, for example, Bruce & Cowley 1981). Accordingly, the dynamical critical exponent is $z = 2$ for elastic transitions (with $m < d$), as in mean-field theory (§ 3), in contrast to the distortive case where typically $z = 2 + c\eta$ with $\eta > 0$. Elastic instabilities may actually be driven by the softening of an optical mode which is linearly coupled to the transverse acoustic phonons; but even in that situation the ensuing critical behaviour turns out to be classical; nevertheless, an anomaly is found in the sound attenuation coefficient (§ 4).

We remark that the anisotropic Hamiltonian (2.4) applies also to spin reorientation transitions (Hornreich & Shtrikman 1976), to the phason instability at $T = 49$ K in TTF-TCNQ (Bak 1976), and to the transition from smectic-A to smectic-C in

a magnetic field (Hornreich & Shtrikman 1977). Anisotropic interactions are also present at Lifshitz points (Hornreich *et al.* 1975).

The phenomenon of local order parameter condensation, induced by defects which locally increase the transition temperature, is qualitatively similar for both distortive and elastic phase transitions. However, dynamically the mechanism of condensation is quite different; while in the distortive case there appear localized modes below the continuum, which then soften at the local transition temperature T_c^l, there appears no such additional localized mode in the elastic case. Instead, the disorder leads to localized vibrational components in the propagating modes, which then 'condense' at T_c^l to form the defect-induced order parameter clusters (§ 5 *a*). As was explained in § 5 *b*, in a system with finite disorder concentration n_D a true defect-induced phase transition can occur at $T_c(n_D)$, resulting in a low-temperature state characterized by an initially strong spatial inhomgeneity, which finally becomes smoothened out at low temperatures, where the disorder influence is suppressed (§ 5 *b*). A dynamical precursor for this singularity at $T_c(n_D)$ (or T_{ord}) is the appearance of a dynamical central peak in the critical region, which only in the case of distortive transitions can be traced back to the softening of a separate phonon impurity band. In the low-temperature phase, besides the new Bragg peaks an additional elastic Huang scattering component emerges as a consequence of the spatial variations of the local order parameter in either case. Near the transition temperature T_c^0 of the pure system, thermodynamic quantities like the order parameter susceptibility and the specific heat appear characteristically rounded. Both these features have been observed in a variety of experiments.

As was discussed in § 2, elastic instabilites often lead to first-order phase transitions, as is the case for the interesting class of martensitic transformations. These materials display a considerably more complex behaviour than the second-order transitions we have discussed here (the precursor effects in martensitic materials are reviewed in Finlayson (1983)). However, a simplifying elastic Ginzburg–Landau free energy has been proposed (Falk 1980, 1983), which is of the form (2.1), but with a negative fourth-order term and including a sixth-order term in order to describe a first-order transition. Recently, an explanation for the experimentally observed 'tweed' pattern in microscopic images of martensitic materials for temperatures far above the transition temperature has been suggested on a similar basis (Kartha *et al.* 1991, 1995; Sethna *et al.* 1992). Namely, such pseudo-periodic lattice deformations were found to emerge in an elastic model including defects that locally modify the transition temperature in a random manner. This intrinsic compositional disorder was found to conspire with the natural geometric constraints of the lattice to form a frustrated glassy 'tweed' phase; and the random order parameter orientations then produce a static central peak with finite width in momentum space. We finally note that an interesting and wide field not covered in the present brief review concerns orientational glasses found in mixed-crystal solids (Höchli *et al.* 1990).

Solid-state physics in recent years has gone beyond the mere study of the materials offered by our surrounding nature, but more and more aims at the creation of new materials with tailored properties. As in semiconductor physics and magnetism, a similar development is about to take place in ferroelastic and ferroelectric substances. Besides of in-depth studies of disorder, the investigation of artificial multilayers and other composite structures will be of importance in the future.

U.C.T. acknowlegdes support from the Deutsche Forschungsgemeinschaft (DFG) under Contract Ta. 177/1-2.

PHILOSOPHICAL TRANSACTIONS OF THE ROYAL SOCIETY A MATHEMATICAL, PHYSICAL & ENGINEERING SCIENCES

References

Aubry, S. & Pick, R. 1971 Soft-modes in displacive transitions. *J. Physique.* **32**, 657–670.

Bak, P. 1976 Phason instability in tetrathiafulvalene-tetracyanoquinodimethane (TTF-TCNQ). *Phys. Rev. Lett.* **37**, 1071–1074.

Bergman, D. J. & Halperin, B. I. 1976 Critical behavior of an Ising model on a cubic compressible lattice. *Phys. Rev.* B **13**, 2145–2175.

Bleif, H., Dachs, H. & Knorr, K. 1971 Diffuse X-ray scattering and change of the lattice parameters of NaOH at the transition from the orthorhombic to the monoclinic phase. *Solid St. Commun.* **9**, 1893–1897.

Brody, E. M. & Cummins, H. Z. 1974 Brillouin-scattering study of the elastic anomaly in ferroelectric KH_2PO_4. *Phys. Rev.* B **9**, 179–196.

Bruce, A. D. & Cowley, R. A. 1981 *Structural phase transitions.* London: Taylor & Francis.

Brugger, K. 1965 Pure modes for elastic waves in crystals. *J. Appl. Phys.* **36**, 759–768.

Bulenda, M., Schwabl, F. & Täuber, U. C. 1996 Defect-induced condensation and central peak at elastic phase transitions. *Phys. Rev.* B **54**, 6210–6221.

Clapp, P. C. 1973 A localized soft mode theory for martensitic transformations. *Phys. Stat. Sol.* B **57**, 561–569.

Clapp, P. C. 1979 Localized soft modes and ultrasonic effects in first order displacive transformations. *J. Mater. Sci. Eng.* **38**, 193–198.

Clapp, P. C. 1981 Pretransformation effects of localized soft modes on neutron scattering, acoustic attenuation, and Mössbauer resonance measurements. *Metall. Trans.* A **12**, 589–594.

Cowley, R. A. 1976 Acoustic phonon instabilities and structural phase transitions. *Phys. Rev.* B **13**, 4877–4885.

Cummins, H. Z. 1982 Brillouin scattering studies of phase transitions in crystals. In *Light scattering near phase transitions* (ed. H. Z. Cummins & A. P. Levanyuk), pp. 359–447. Amsterdam: North Holland.

Errandonéa, G. 1981 Brillouin scattering observations of centrals peaks in ferroelastic LaP_5O_{14}. *Ferroelectrics* **36**, 423–426.

Falk, F. 1980 Model free energy, mechanics, and thermodynamics of shape memory alloys. *Acta Metall.* **28**, 1773–1780.

Falk, F. 1983 Ginzburg–Landau theory of static domain walls in shape-memory alloys. *Z. Phys.* B **51**, 177–185.

Finlayson, T. R. 1983 Structural transformations and their precursors. *Aust. J. Phys.* **36**, 553–563.

Fleury, P. A. & Lyons, K. B. 1982 Central peaks near structural phase transitions. In *Light scattering near phase transitions* (ed. H. Z. Cummins & A. P. Levanyuk), pp. 449–502. Amsterdam: North Holland.

Folk, R. & Schwabl, F. 1974 EPR in $SrTiO_3$: dynamical or dirt effect? *Solid St. Commun.* **15**, 937–940.

Folk, R., Iro, H. & Schwabl, F. 1976*a* Elastic phase transitions of second order. *Phys. Lett.* **57A**, 112–114.

Folk, R., Iro, H. & Schwabl, F. 1976*b* Critical statics of elastic phase transitions. *Z. Phys.* B **25**, 69–81.

Folk, R., Iro, H. & Schwabl, F. 1977 Critical dynamics and statics of uniaxial dipolar magnets. *Z. Phys.* B **27**, 169–175.

Folk, R., Iro, H. & Schwabl, F. 1979 Critical dynamics of elastic phase transitions. *Phys. Rev.* B **20**, 1229–1244.

Fox, D. L., Scott, J. F. & Bridenbaugh, P. M. 1976 Soft modes in ferroelastic LaP_5O_{14} and NdP_5O_{14}. *Solid St. Commun.* **18**, 111–113.

Garland, C. W., Park, G. & Tatsuzaki, I. 1984 Ultrasonic attenuation and critical relaxation rates in $KH_3(SeO_3)_2$ and $KD_3(SeO_3)_2$. *Phys. Rev.* B **29**, 221–225.

Halperin, B. I. & Varma, C. M. 1976 Defects and the central peak near structural phase transitions. *Phys. Rev.* B **14**, 4030–4044.

PHILOSOPHICAL TRANSACTIONS OF THE ROYAL SOCIETY A MATHEMATICAL, PHYSICAL & ENGINEERING SCIENCES

Haussühl, S. 1973 Anomalous thermoelastic behaviour of cubic potassium cyanide. *Solid St. Commun.* **13**, 147–151.

Höchli, U. T., Knorr, K. & Loidl, A. 1990 Orientational glasses. *Adv. Phys.* **39**, 405–615.

Höck, K. H. & Thomas, H. 1977 Statics and dynamics of 'soft' impurities in a crystal. *Z. Phys.* B **27**, 267–271.

Höck, K. H., Schäfer, R. & Thomas, H. 1979 Dynamics of a locally distorted impurity in a host crystal with displacive phase transition. *Z. Phys.* B **36**, 151–160.

Hornreich, R. M., Luban, M. & Shtrikman, S. 1975 Critical behavior at the onset of k-space instability on the λ line. *Phys. Rev. Lett.* **35**, 1678–1681.

Hornreich, R. M. & Shtrikman, S. 1976 On the critical behaviour of spin-reorientation phase transitions. *J. Phys.* C **9**, L683–L686.

Hornreich, R. M. & Shtrikman, S. 1977 Critical behavior of the smectic-A to C phase transition in a magnetic field. *Phys. Lett.* **63A**, 39–41.

Kartha, S., Castán, T., Krumhansl, J. A. & Sethna, J. P. 1991 Spin-glass nature of tweed precursors in martensitic transformations. *Phys. Rev. Lett.* **67**, 3630–3633.

Kartha, S., Krumhansl, J. A., Sethna, J. P. & Wickham, L. K. 1995 Disorder-driven pretransitional tweed pattern in martensitic transformations. *Phys. Rev.* B **52**, 803–822.

Khmel'nitskii, D. E. 1975 Critical phenomena in deformation phase transitions. *Sov. Phys. Solid St.* **16**, 2079–2080 (1974 *Fiz. Tverd. Tela* **16**, 3188–3190).

Knorr, K., Loidl, A. & Kjems, J. K. 1985 Continuous ferroelastic phase transition of a KBr:KCN mixed crystal. *Phys. Rev. Lett.* **55**, 2445–2448.

Krumhansl, J. A. 1968 Some considerations of the relation between solid state physics and generalized continuum mechanics. In *Proc. IUTAM Symp. on Mechanics of Generalized Continua* (ed. E. Kröner), pp. 298–311. Berlin: Springer.

Kunin, I. A. 1968 The theory of elastic media with microstructure and the theory of dislocations. In *Proc. IUTAM Symp. on Mechanics of Generalized Continua* (ed. E. Kröner), pp. 321–329. Berlin: Springer.

Leibfried, G. & Ludwig, W. 1961 Theory of anharmonic effects in crystals. In *Solid state physics* (ed. F. Seitz & D. Turnbull), vol. 12, pp. 275–444. New York: Academic.

Liakos, J. K. & Saunders, G. A. 1982 Application of the Landau theory to elastic phase transitions. *Phil. Mag.* A **46**, 217–242.

Lüthi, B. & Rehwald, W. 1981 Ultrasonic studies near structural phase transitions. In *Structural phase transitions I* (ed. K. A. Müller & H. Thomas), pp. 131–184. Berlin: Springer.

Mindlin, R. D. 1968 Theories of elastic continua and crystal lattice theories. In *Proc. IUTAM Symp. on Mechanics of Generalized Continua* (ed. E. Kröner), pp. 312–320. Berlin: Springer.

Morgenstern, M. 1988 Der Einfluß von stochastischen Feldern auf das kritische Verhalten anisotroper Systeme. Dissertation, Technische Universität München.

Müller, K. A. 1979 Intrinsic and extrinsic central-peak properties near structural phase transitions. In *Dynamical critical phenomena and related topics* (ed. C. P. Enz), pp. 210–250. Berlin: Springer.

Poniatovskii, E. G. 1958 The critical point in the polymorphic transformation curve of cerium. *Sov. Phys. Dokl.* **3**, 498–500 (1958 *Dokl. Akad. Nauk. SSR* **120**, 1021–1024).

Rae, A. I. M. 1978 The structural phase change in s-triazene. III Lattice energy calculations. *J. Phys.* C **11**, 1779–1785.

Rao, C. N. R. & Rao, K. J. 1987 *Phase transitions in solids.* New York: McGraw-Hill.

Rehwald, W., Rayl, M., Cohen, R. W. & Cody, G. D. 1972 Elastic moduli and magnetic susceptibility of monocrystalline Nb_3Sn. *Phys. Rev.* B **6**, 363–371.

Riste, T., Samuelsen, E. J., Otnes, K. & Feder, J. 1971 Critical behaviour of $SrTiO_3$ near the 105 K phase transition. *Solid St. Commun.* **9**, 1455–1458.

Rowe, J. M., Rush, J. J., Vagelatos, N., Price, D. L., Hinks, D. G. & Susman, S. 1975 Crystal dynamics of KCN and NaCN in the disordered cubic phase. *J. Chem. Phys.* **62**, 4551–4554.

Salje, E. K. H. 1992 Application of Landau theory for the analysis of phase transitions in minerals. *Phys. Rep.* **215**, 49–99.

PHILOSOPHICAL TRANSACTIONS OF THE ROYAL SOCIETY A MATHEMATICAL, PHYSICAL & ENGINEERING SCIENCES

Sasvári, L. & Schwabl, F. 1982 Critical dynamics in the presence of relaxing defects. *Z. Phys.* B **46**, 269–283.

Schmidt, H. & Schwabl, F. 1977 Localized modes and central peak at displacive phase transitions. *Phys. Lett.* **61A**, 476–478.

Schmidt, H. & Schwabl, F. 1978 Localized defects in a one-dimensional Ginzburg–Landau model. *Z. Phys.* B **30**, 197–210.

Schwabl, F. 1980 Elastic phase transitions. *Ferroelectrics* **24**, 171–178.

Schwabl, F. 1985 Propagation of sound at continuous structural phase transitions. *J. Stat. Phys.* **39**, 719–737.

Schwabl, F. & Täuber, U. C. 1991*a* Elastic phase transitions in inhomogeneous media. *Phase Transitions* **34**, 69–103.

Schwabl, F. & Täuber, U. C. 1991*b* Defect-induced condensation and central peak at structural transitions. *Phys. Rev.* B **43**, 11 112–11 135.

Sethna, J. P., Kartha, S., Castán, T. & Krumhansl, J. A. 1992 Tweed in martensites: a potential new spin glass. *Phys. Scr.* T **42**, 214–219.

Shapiro, S. M., Axe, J. D., Shirane, G. & Riste, T. 1972 Critical neutron scattering in $SrTiO_3$ and $KMnF_3$. *Phys. Rev.* B **6**, 4332–4341.

Shirane, G. & Axe, J. D. 1971 Acoustic-phonon instability and critical scattering in Nb_3Sn. *Phys. Rev. Lett.* **27**, 1803–1806.

Smith, J. M. & Rae, A. I. M. 1978 The structural phase change in s-triazene. I The crystal structure of the low-temperature phase. *J. Phys.* C **11**, 1761–1770.

Villain, J. 1970 Self consistency of Landau's model in the transition from piezo- to ferroelasticity. *Solid St. Commun.* **8**, 295–297.

Wadhawan, V. K. 1982 Ferroelasticity and related properties of crystals. *Phase Transitions* **3**, 3–103.

Wegner, F. J. 1974 Magnetic phase transitions on elastic isotropic lattices. *J. Phys.* C **7**, 2109–2125.

Weyrich, K. H. & Siems, R. 1984 Molecular dynamics calculations for systems with a localized 'soft-mode'. *Ferroelectrics* **55**, 333–336.

Wiesen, B., Weyrich, K. H. & Siems, R. 1987 Anharmonic dynamics of defect pairs in soft-mode systems. *Phys. Rev.* B **36**, 3175–3181.

Wiesen, B., Weyrich, K. H. & Siems, R. 1988 Dynamics of localized clusters in soft mode systems. *Ferroelectrics* **79**, 69–72.

Yamaguchi, M., Inoue, K. & Yagi, T. 1995 Soft acoustic mode in the ferroelectric phase transition of hexagonal barium titanate. *Phys. Rev. Lett.* **74**, 2126–2129.

PHILOSOPHICAL TRANSACTIONS OF THE ROYAL SOCIETY A MATHEMATICAL, PHYSICAL & ENGINEERING SCIENCES